SERUM microRNA 362-3p aS A POTENTIAL BIOMARKER TO PREDICT THE EXTENT OF DRUG-INDUCED QT INTERVAL LENGTHENING AMONG HEART FAILURE PATIENTS

by

Rakan Jamal Alanazi

A Thesis

Submitted to the Faculty of Purdue University

In Partial Fulfillment of the Requirements for the degree of

Master's of Science

Department of Pharmacy Practice

West LafayetteWest Lafayette, Indiana

December 2020

THE PURDUE UNIVERSITY GRADUATE SCHOOL
STATEMENT OF COMMITTEE APPROVAL

Dr. Brian R. Overholser, Chair
Department of Pharmacy Practice

Dr. James E. Tisdale
Department of Pharmacy Practice

Dr. Kevin M. Sowinski
Department of Pharmacy Practice

Approved by:
Dr. Brian R. Ovehrolser

ACKNOWLEDGMENTS

I want to express my appreciation to my primary mentor, Dr. Overholser. His enthusiasm and support have seen me throughout my entire academic training. I especially appreciate the great time he spent guiding me on developing every part of my research skills. Most importantly, the patience he showed me encouraged me and made me feel confident as I completed my M.S thesis.

Besides my primary mentor, I would like to express my appreciation for my graduate committee. Without them, it would have been challenging to complete my training throughout my M.S degree. I truly owe them this success. Each member of my thesis committee has offered me extensive personal and professional guidance. My sincere thanks go to Drs. Tisdale and Sowinski for their insightful comments and encouragement. I am thankful for their support that motivated me. I would also like to extend my sincere gratitude to Dr. Michael A. Heathman in the Division of Clinical Pharmacology at the Indiana University School of Medicine for his assistance using Nonlinear Mixed Effects Modeling (NONMEM) software. His contribution was critical toward the completion of my project.

I also owe a great deal of gratitude to my graduate colleagues in the Purdue Department of Pharmacy Practice for their continued support throughout my time. Finally, I would like to thank my parents for their support and encouragement

TABLE OF CONTENTS

LIST OF TABLES

LIST OF FIGURES

ABSTRACT

Background: The sensitivity to drug-induced QT prolongation is highly variable in heart failure (HF) patients. QT interval prolongation can lead to a life-threatening ventricular arrhythmia known as torsade de Pointes (TdP), which can result in sudden cardiac death. Although QT prolongation is a surrogate marker for sudden cardiac death, the extent of drug-induced QT prolongation, and thus TdP, is largely unpredictable. Therefore, developing a biomarker to predict patients' sensitivity to drug-induced QTc prolongation could have a profound clinical impact. MicroRNA (miR) are recognized as important regulators of cardiovascular function as they shape the transcriptome by targeting mRNAs for repression of translation. Our multidisciplinary research group has demonstrated that miR-362-3p regulates a potassium channel (i.e., hERG) that is the most widely implicated in drug-induced QTc prolongation. The primary objects of this analysis focus on characterizing serum miR-362-3p expression in the circulation as a potential biomarker to predict subject's susceptibility to ibutilide exposure induced QT-interval prolongation

Methods: The dataset utilized to develop the PK-PD models were collected from a previous clinical study carried out by Tisdale et al. (Tisdale, et al. 2020). A total of 22 adult subjects who met the inclusion and exclusion criteria were enrolled and divided into three groups: a group of patients with heart failure with preserved ejection fraction (HFpEF, n=10), a group of patients with heart failure with reduced ejection fraction (HFrEF, n=2), and ten healthy subjects in the control group who were matched to subjects in the HFpEF group for age and sex. Following a baseline day of triplicate 12-lead ECGs, all subjects received ibutilide 0.003 mg/kg intravenously infused over 10 minutes. Serial collection of blood samples to determine serum Ibutilide concentrations (HPLC/MS), serum miR-362-3 expression (qPCR), with triplicate ECG readings were obtained pre-and-post ibutilide administration. To describe ibutilide serum concentration exposure and the

relationship with Fridericia-corrected QT (QTF) intervals, a non-linear mixed effect modeling approach was used along with clinical and demographic data, and serum miR-362-3p expression was evaluated as potential covariates on the PK/PD model.

Results: A three-compartment model best described the time course of ibutilide concentrations profile with a proportional residual error. The individual ibutilide concentrations time profile was then used in an indirect response model where ibutilide concentrations are indirectly driving the QT interval prolongation through inhibition of the output (Kout) parameters linked to an indirect response model with zero-order input parameter best described the ibutilide concentrations QT interval lengthening relationship. The Individual PK/PD parameters using the base model for the Imax and IC50 were 11.4% (9.9% RES) and 0.36 (8.4% RES) ng/mL, respectively. Following stepwise forwarding inclusion steps, the final covariate analyses identified circulating miR-362-3p expression associated with a history of myocardial infarction covariate influencing both the Imax and IC50 ($p<0.05$).

Conclusions: An indirect response model has been developed to describe the effects of ibutilide concentrations on QT-intervals. Although the semi-mechanistic model could not be developed; serum miR-362-3p expression was identified as a significant predictor for ibutilide-induced QT-interval prolongation. Moreover, the upregulation of serum miR-362-3p expression enhanced IC50 seen after ibutilide administration. The potential use of miR-362-3p as a biomarker warrants further investigation to identify patients at the greatest risk of TdP.

CHAPTER 1. INTRODUCTION

1.1 QT Interval

The QT interval on the electrocardiogram (ECG) represents the duration from the QRS complex's onset to completing the T wave. It encompasses the time required for the ventricular myocytes to repolarize after depolarization. (Thomas, et al. 1996) The 99th percentiles for QTc interval prolongation in men and women are >470 and >480 ms, respectively, have been recommended as definitions of QTc prolongation. (Drew, et al. 2010)

1.1.1 Correction Method for the QT Interval

The QT interval is affected by changes in heart rate, and so formulas must be used to correct the QT interval for heart rate. The patient's heart rate and QT interval are used to calculate a corrected QT (QTc) interval value. (Rabkin, et al. 2015; Rabkin, et al. 2017) Several formulas have been proposed for QT interval corrections (QTc) for changes in heart rate. (Bazett,et al. 1920; Fridericia, et al. 1920; Sagie,et al. 1992; Rautaharju,et al.2004; Rabkin,et al. 2015) There is not a "gold standard" among the formulas. However, the most commonly studied and applied QTc formulas are the Bazett, Fridericia, Framingham, and Rautaharju. (Indik, et al.2006; Vandenberk, et al. 2016; Rabkin, et al. 2017) The Bazett formula is the most extensively used correction method in clinical practice, and the United States Food and Drug Administration (FDA) has recommended the Fridericia formula for clinical trials on drug safety. (Phan, et al. 2015)

In 1920, Henry Cuthbert Bazett proposed the Bazett formula (Eq. 2). The formula performs best with a heart rate range of 60–100 beats/min. (Bazett, et al. 1920) However, the formula is criticized because of its inaccuracy as it was only derived from 39 subjects and overcorrects the measured QT interval at heart rates > 100 bpm and under corrects at heart rates <60 bpm. (Sagie,

et al. 1992) Despite the critics, the Bazett formula remains a frequently used correction approach. (Manion, et al. 1985; Sage, et al. 1992) It is still widely used because the thresholds for torsades de pointes risk have been determined using Bazett's formula (> 500 ms for marked increase risk of torsade de pointes (TdP); >470 in men and >480 in women for QTc prolongation. (Rautaharju, et al. 2009)

$$QTcB = \frac{QT}{\sqrt{RR}} \quad (1)$$

where QTcB = the Bazett's correct QT interval and RR is the ventricular rate

The Framingham formula (QTcFra) was proposed by Sagie et al. in 1992 and was supported by a study of approximately 5000 patients from the Framingham population in the USA. (Sagie, et al. 1992) This linear equation (Eq. 2) gave a more uniform QTc over a broader range of heart rates and is considered a better and preferred formulas then Bazett's. (Vandenberk, et al. 2016) However, the Framingham formula is inconvenient for use at the bedside. (Luo, et al. 2004)

$$QTcFra = QT + 0.154(1 - RR) \quad (2)$$

The Fridericia formula was derived by Louis Sigurd Fridericia in 1920 from observations of 50 healthy subjects aged 3 to 81 years. Fridercia found that taking the cube root of the RR interval gave the best adjustment formula in comparison to Framingham. The formula (Eq. 3) provides more accurate QTc values in subjects with tachycardia but has the same limitations as Bazett's formula for slow heart rates. (Rautaharju, et al. 2002) Bazett's and Fridercia's formulas are logarithmic corrections. (Fridericia, et al. 1920)

$$QTcFri = \frac{QT}{\sqrt[3]{RR}} \quad (3)$$

1.2 Electrophysiology of Ventricular Repolarization

The QT interval measured on the ECG indicates the total duration of the ventricular electrical systole and diastole. The QT interval includes the ventricular depolarization time (indicated by the QRS duration) and the repolarization time (indicated by JT interval and the T wave). (Figure 1) The transition of ventricular depolarization into ventricular repolarization conforms to the J-point on a standard ECG. (Gussak, et al. 1995) To appreciate the role of the QT interval in evaluating ventricular repolarization, it is of utmost importance to understand the role of the cardiac action potent al and the major ion channels involved in the process

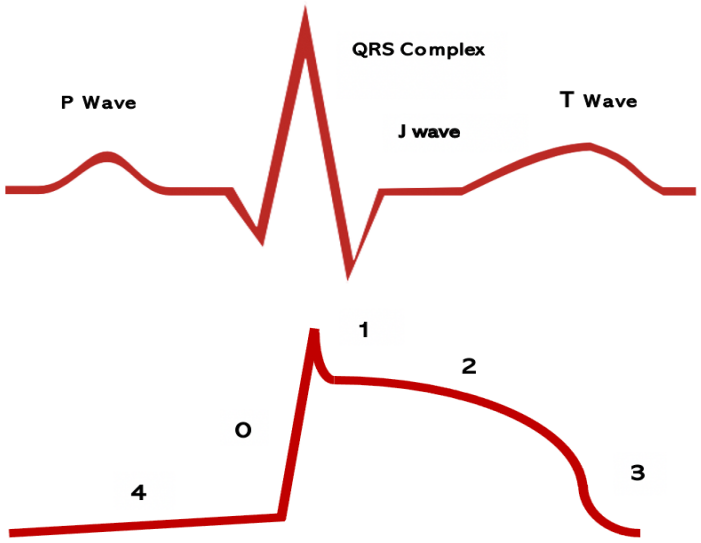

Figure 1. illustrations of Action Potential Corresponded to Electrocardiogram (ECG)

Panels (A) displays the surface of ECG waveform, P wave represents depolarization of the atria; the QRS complex represents the depolarization of the ventricles, and the T Wave represent rapid repolarization; Panels (B) display the ventricular action potential to the surface of ECG (Panel A); phase 0 represents the ventricular depolarization mediated by Na+ channel activation; phase 1 represents early rapid repolarization due to transient outward movement of K+; phase 2 represent plateau phase determined by the movement of inward Ca^{2+}/Na^{+}; phase 3 represents the late repolarization due to movement of K+, and phase 4 represents the resting phase maintained by the Na /K+ pump.

All mammalian cardiac cells have channels embedded in the plasma membrane to allow for the inward and outward movement of ions in the cells. These cardiac ion channels are essential in shaping the action potential. The channels may be open, closed, or inactivated depending on changes in cardiac membrane potential. Ventricular depolarization occurs as a result of the coordination of action potentials, whereas repolarization occurs as a result of the recovery and return of membrane potential to the baseline resting phase. (Lester, et al. 2019)

The essential ions responsible for the membrane potential are Na^+, K^+, Ca^{2+}, and Cl^-. The intracellular concentration of K^+ is higher, and the concentration of Na^+, Ca^{2+}, and Cl^- are higher outside the cell. (Klabunde, et al. 2017) In a normal cardiac cycle, there is an inward flow of positive ions (mainly sodium and calcium currents) activating depolarization and outward movement of positive ions (mainly potassium currents) activating repolarization. There are five distinct phases (0 through 4) to the cardiac action potential, as described below, the start and end being the baseline resting phase (4) (Locati, et al. 2017).

- Phase 0 (Rapid depolarization): A sudden influx of Na^+ ions (I_{Na}) through Na^+ channels produces an abrupt spike of the action potential.
- Phase 1 (Notch or rapid repolarization): A partial repolarization following rapid depolarization due to closure of Na+ channels and the temporary outward movement of K^+ (I_{to}) via the K^+ channels.
- Phase 2 (Plateau): The cardiac muscle fiber is in the depolarized state. There is a balance of Ca^{2+} (I_{Ca}) inward via the opening of L-type Ca^{2+} channels, and Na_inward via $I_{Na,}$ channels and the closure of rectifier K^+ channels.

- Phase 3 (Repolarization): Cardiac repolarization primarily occurs due to the K^+ efflux through delayed rectifier current (I_{Kr} and I_{Ks}). I_{Kr} is the current primarily responsible for ventricular repolarization.
- Phase 4 (Diastolic): The resting membrane potential or polarized state is maintained by the sodium-potassium ATPase pump, Na^+/Ca^{2+} exchanger, and the inward rectifier K^+ current (I_{K1}).

Any changes in phase 3 occurring in the absence of dispersion of depolarization are considered a primary reason for QT prolongation, which indicates a lengthening of the refractory period of cardiac tissue. QT prolongation may be associated with blockade or modification of K^+ efflux through delayed rectifier currents (I_{Kr} and I_{Ks}). (Roden, et al. 2008) A fundamental assumption in the interpretation of cardiac electrophysiology states that a QT prolongation is secondary to an increased action potential duration in at least a few regions of the ventricle. This increase in action potential duration, in turn, indicates a decrease in outward current or an increase in inward current (Keating, et al. 2001).

1.3 Drug-Induced QTc Prolongation and TdP

Prolongation of the QT/QTc can lead to a potentially deadly ventricular arrhythmia known as Torsade de Pointes (TdP), which was s first described by the French physician Francois Dessertenne in 1966. (Dessertenne, et al. 1966) Torsade de Pointes is an unusual polymorphic ventricular tachycardia characterized by a continuously changing amplitude and the twisting appearance of the QRS complexes around the isoelectric line on an ECG, that first appear positive and then negative. (Drew, et al. 2010) The mechanism of the relationship between the duration of the QT interval and the risk of TdP remains inconclusive. However, in general a QTc of higher

than 500 ms or an increase in the QTc interval greater than 60 ms is usually considered to confer a high risk of TdP in an individual patient. (Heist, et al. 2005, Barnes, et al. 2010)

1.3.1 Risk Factors for Drug-Induced QTc Interval Prolongation

Major factors influencing the prevalence of QTc interval prolongation and TdP include QT-prolonging drug therapy, electrolyte abnormalities (e.g., a decrease in serum potassium and decrease in serum magnesium and calcium), and genetic polymorphisms that increase TdP risk. Other evident risk factors include a QTc interval >500 ms, a ≥60 ms increase in QTc interval from the pretreatment value, female sex (females have a two-fold increased risk compared to males), advanced age, heart failure with reduced ejection fraction, acute myocardial infarction, bradycardia, use of diuretics, inadequate dose adjustment of renally eliminated drugs in patients with kidney disease, elevated plasma concentrations of QTc interval prolonging drugs caused by drug interactions, and rapid intravenous administration of high-risk drugs. (Tisdale, et al. 2016) Also, the multiplicity of risk factors further raises a patient's risk of TdP, and if not properly managed, TdP can progress to ventricular fibrillation (VF) or sudden cardiac death (SCD). (Li, et al. 2010)

Abnormal QT/QTc prolongation is of two categories, congenital (cLQTS) and acquired (aLQTS). The congenital form was first described in 1975 and is a relatively uncommon but crucial clinical disorder. Congenital Long-QT syndrome is subdivided based on the underlying gene in which causative mutations occur. The most common forms are LQT1, LQT2, and LQT3 which are associated with the genes KCNQ1, KCNH2, and SC5NA, respectively. The clinical manifestations of LQT syndrome involve syncopal episodes, which can, albeit uncommonly, include sudden death due to cardiac arrest. It has been demonstrated that QTc-prolonging drugs

increase the risk of SCD in LQT patients up to two to eight times. (Straus, et al. 2005; Straus , et al. 2006)

1.3.2 Drug-Induced QTc Interval Lengthening in Patients with Heart Failure

Patients with heart failure (HF) are at a threefold increased risk of developing TdP. (Lo, et al. 2008) As heart failure progresses, there are alterations in the expression and function of several ion channels, including downregulation of KCNH2. (Beuckelmann,et al. 1993, Nabauer, et al. 1993, Tomaselli, et al. 1999) The KCNH2 gene, also referred to as the human Ether-a-go-go Related Gene (i.e. hERG), encodes a potassium channel responsible for the rapid component of the delayed rectifier K+ current (I_{Kr}) in the heart. (Sanguinetti, et al. 1995) I_{Kr} is crucial for ventricular repolarization and inhibition of this current prolongs the QT interval on a surface ECG which can influence the development of TdP. (Vandenberg, et al., Perry, et al. 2012) Even alterations in the KCNH2 function that do not present as QT interval prolongation can increase susceptibility to arrhythmias by increasing the dispersion of repolarization or by the depletion of the repolarization reserve. (Wu, et al. 2009, Yasuda et al. 2015) The term repolarization reserve refers to the redundancy of outward currents that drive repolarization. In addition to I_{Kr}, the slow component of the delayed rectifier current (I_{Ks}), contributes to ventricular repolarization, particularly during rapid heart rates or when I_{Kr} is compromised. Consequently, the decrease of a single outward potassium current, such as I_{Kr}, may not lead to noticeable changes in QT-interval.

1.4 miRNA Biogenesis and Function

Over the last decade, microRNAs (miRNAs or miRs) have been identified to regulate genes important for proper cardiac function. miRNAs are short, 22 base-long segments of non-coding

RNA that are involved in the regulation of gene expression in a wide variety of cellular processes. (Van, et al. 2011) The first miRNA (lin-4) was observed in C. Elegans in 1993. (Lee, et al. 1993)Since then, hundreds of miRNAs have been discovered in several species, particularly emphasizing their role in embryonic development and disease regulation. (Pritchard, et al. 2012) It is now recognized that miRNAs are evolutionarily conserved among species and account for up to 3% of the mammalian genome. (Bartel, et al. 2009)

miRNAs are transcribed by RNA polymerase II to generate a sizeable stem-loop structure called the primary miRNA (pri-miRNA). (Cai, et al. 2004) The stem-loop structure in the nucleus is bound by an RNase Drosha complex and its cofactor Dgcr8, which cleaves the structure to produce the hairpin loop-shaped precursor miRNA. (pre-miRNA)(Denli, et al. 2004) The pre-miRNA is then exported to the cytoplasm by the nuclear transport receptor Exportin5, and the nuclear G-protein Ran-GTP. (Bohnsack, et al. 2004) In the cytoplasm, another RNase known as Dicer cleaves the loop off of the stem-loop structure, thus producing a duplex nucleotide containing miRNA. Finally, one strand from the duplex degenerates, and the other strand is assimilated into the RNA induced silencing complex (RISC) which includes Argonaute, the catalytic unit of the complex. (Schwarz, et al. 2003, Du, et al. 2005) The mature RNA in the RISC complex finds the target mRNA by binding to the 2-8 nucleotide "seed region" at the 3' end of the target mRNA. This results in translational repression or mRNA degradation and hence silences the target gene. (Pasquinelli, et al. 2012) The miRNA-RISC complex interaction with the 3'-untranslated regions (3' UTR) of the target gene to silence gene expression is well accepted. However, many studies have shown that a few miRNAs can also interact with the 5'-UTR (Gu, et al. 2014, Broughton, et al.2016), coding sequences (Brummer, et al. 2014), and can even activate translation. (Xiao, et al. 2017) This interaction is dependent on various factors, including

subcellular localization, miRNA abundance, and the level of complementation of the miRNA-mRNA complex (O'Brien, et al. 2018).

The sequencing of the human genome in 2001 has paved a path for expanded identification of new miRNAs and their target genes. As more miRNAs have been identified, the research focus has shifted towards the functional characterization of miRNAs as they relate to human diseases and developmental anomalies. Many miRNAs have been found to play important roles in critical biological processes, including cell division and death, immunity, signal transduction, metabolism, and cell locomotion (Li, et al. 2012). Given this, the aberrant expression of several miRNAs associated with cancer, viral pathogenesis, and immune dysfunction was not surprising. Among the various conditions, cancer is the most prominent human disease that has a stable association with miRNA mis-regulation. The earliest association was investigated in 2002, wherein the deletion of miR-15 and miR-16 was observed in 65% of patients with B-cell chronic lymphocytic leukemia. (Calin, et al. 2002) Widespread expression profiling studies further strengthened the association with miRNA dysregulation and increased susceptibility to various cancers, most notably, breast cancer and lung cancer. Moreover, miRNA expression patterns have been assessed to pinpoint the cancer progression stages. (Acunzo, et al. 2015) In addition to their substantial role in cancer development and progression, miRNAs have been implicated in degenerative diseases, especially neurodegenerative diseases like Parkinson's and Alzheimer's. (Sharma, et al. 2018) Also, they have been implicated in a variety of other degenerative disorders of bone , (van Wijnen, A. J., et al. 2013), retina (Loscher, et al. 2008), muscle (Wang, et al. 2018), and heart. (Ultimo, et al. 2018)

1.4.1 microRNA & Regulation of Gene Expression

MicroRNAs regulate gene expression by direct base pairing to the 3'UTR region of target transcripts. (Oliveto, et al. 2017) The miR-3'UTR complex disrupts translation by silencing the gene or promoting the degradation of mRNA. The characteristics and function of miRNA and antisense miRNA (anti-miRNA) have been studied as potential therapeutic agents. Anti-miRNA consist of reverse complementary sequences that lower endogenous miRNA expression and enhance gene expression. (Marquez, et al. 2008) Miravirsen is the first anti-miR (inhibits miR-122) that has been FDA approved in patients with viral hepatitis C. (Hu, et al. 2012) Clinical trials have demonstrated that miravirsen is well-tolerated; hence the enthusiasm for developing other anti-miRNA -based drugs has increased.

The distribution of miRNA or anti-miRNA to cardiac muscle tissue remains a challenge due to several physiological and cellular obstacles experienced *en route* to target cells. (Guzman-Villanueva, et al. 2012) Nevertheless, pathophysiological signal targeting mechanisms that enhance miRNA expression may be useful to normalize the expression of gene targets. However, the mechanisms of the physiologic and pathophysiologic regulation of miRNA expression is an underserved area of research. This provides an opportunity for the development of pharmacological inhibitors targeting the regulatory pathways of miRNA in diseases such as HF Furthermore, the circulation of miRNA in the blood makes them attractive as potential biomarkers for clinical diagnosis. (Reid, et al. 2012)

1.4.2 miRNAs in Cardiovascular Function and Anomalies

miRNAs are expressed in cardiovascular tissue and have been identified as regulators of cardiovascular function. In addition to serving an essential role in cardiac development, they play

a role in the pathogenesis of various cardiovascular diseases, including cardiac arrhythmias, myocardial infarction, atherosclerosis, and coronary artery disease. (Romaine, et al. 2015) The cardiac-specific knockout of the endonuclease Dicer, which effectively disrupts all miRNAs, results in severe cardiac developmental anomalies, pericardial edema, and death. (da Costa Martins, et al. 2008) A global genomic study on healthy human heart muscle in 2008 revealed a handful of miRNAs including miR-1, miR-16, miR-27b, miR-30d, miR-126, miR-133, miR-143, miR-208 and let-7 which were found abundantly in cardiac tissue compared to other tissues. Taken together, this suggests that miRNAs have a definite role in cardiac muscle function and maintenance. (Landgraf,et al. 2007, Thum, et al. 2008) Current research has revealed more specific functions for these miRNAs, along with the identification of newly associated miRNAs in cardiac disease. For example, miR-1 has been identified as an indicator of an increased risk for heart failure development. (Sygitowicz, et al. 2015) Additionally, miR-126 is upregulated in response to vascular injury of the heart and is crucial for cell proliferation and maintenance. (Chistiakov, et al. 2016) Any loss of its expression has been associated with atrial fibrillation and heart failure due to loss of its protective function against cardiac hypoxia. (Wei, et al. 2015)

1.4.3 Dysregulations of miRNA in Patients with Heart Failure

There is increasing evidence suggesting that miRNA dysregulation is associated with heart failure and comorbid pathological conditions. Both miR-1 and miR-210 regulation are positively correlated with New York Heart Association (NYHA) functional classifications. (Endo, et al. 2013, Sygitowicz, et al. 2015, Zhou, et al. 2018) In addition, decreased expression of the miRNAs let-7i, miR-18b, miR- 18a, miR-223, miR-301a, miR-652, and miR-423 are correlated with increased risk of mortality in HF patients. (Ovchinnikova, et al. 2016) Contrarily, increased levels of miR-1254 and miR- 1306 are correlated with hospitalization and death, and increased levels of

miR-208b and miR- 499 are strongly correlated with the development of HF and death. (Bayes-Genis, et al. 2018)

The screening and examination of miRNA expression profiles in healthy and failing human hearts has been accomplished with deep sequencing and bioinformatics. Around 250 miRNAs were differentially expressed in failing human hearts compared to that of controls; high expression of miRNAs was observed in patients with refractory end-stage heart failure. (Leptidis, et al. 2013)

1.4.4 miR-362-3p Targets KCNH2

The mechanism for downregulation of KCNH2 during heart failure and the potential role of miR regulation is unknown. Our laboratory has correlated five miRs with KCNH2 mRNA down-regulation and increased in patients with a single nucleotide polymorphism (SNP) linked to QT interval lengthening. (Shao M, et al. 2013) Through *in vitro* and *ex vivo* examination, miR-362-3p has been identified as binding to the 3'UTR region of KCNH2, resulting in decreased KCNH2-mRNA and protein expression leading to lower I_{Kr} density. (Assiri, et al. 2019)

miR-362-3p is endogenously expressed in the heart, and further deep sequencing showed that it is upregulated during cardiac hypertrophy. (Leptidis, et al. 2013) It has also been suggested that miRNAs may be promising biomarkers in the diagnosis HF both in patients with reduced ejection fraction (HFrEF) and with preserved ejection fraction (HFpEF). (Schulte, et al. 2015)

Interestingly, our laboratory has demonstrated that miR-362-3p is upregulated in cardiac tissue during HFrEF. (Mourad, et al. 2015) The ventricular tissue of patients with HFrEF demonstrated a 60% increase in miR-362-3p coupled with a 40% reduction in KCNH2 expression. These data support that increased expression of miR-362-3p downregulates KCNH2 to increase the susceptibility to arrhythmias during HFrEF. Overall, there is clear evidence to advocate the

crucial role of miRNAs in heart failure pathogenesis and their use as a potential biomarker in heart failure therapy.

1.5 Population Pharmacokinetics Pharmacodynamic Model Concept

Population pharmacokinetic (PK) and pharmacodynamics (PD) modeling techniques assist in the identification of inter-and intra-individual variability that affects drug safety and efficacy. (Sun, et al. 1999) Sheiner first introduced the PK modeling concept in 1972. Initially, PK modeling was developed to assess sparse drug concentration data collected during therapeutic drug monitoring, (Sheiner, et al. 1980) but later expanded to include a PKPD modeling relationship.The term population pharmacokinetics refers to the 'mixed-effects' (parameterization) modeling, a mixture of fixed and random effects. (Aarons, et al. 1991) According to Mould et al., (Mould, et al. 2012) population pharmacokinetics is "the study of pharmacokinetics at the population level, in which data obtained from all individuals in a population are evaluated simultaneously using a non-linear mixed-effects model."

Traditional PK studies are designed with a detailed sampling schedule and collect multiple samples at fixed intervals. On the other hand, the population PK method is designed to include sparse sampling schedules but in a larger number of patients. These patients are usually given similar or different doses of drugs, and blood samples from these patients are taken from different time intervals. (Charles, et al. 2014) Pharmacokinetic modeling is an essential part of drug development and is an extensive investment for new therapeutic agents. As such, PK assessment involves a complex process requiring the rigorous procedures necessary to provide orderly data, appropriate computing platforms, adequate resources, and effective delivery. (Mould, et al. 2012)

1.5.1 Non-linear Mixed-effects Modeling Concept

The term population PK usually refers to' mixed-effects models' (parameterization), a combination of fixed and random effects. Parameters that do not differ across individuals are known as fixed effects (structural). In contrast, the random effects parameters that vary across individuals may include inter-subject variability, which may account for the remaining unexplained variation. (Mould, et al. 2012, Charles, et al. 2014)

1.5.2 Aspects of PK/PD Modeling

There are four key sequential processes generally required to develop population pharmacokinetic/ pharmacodynamics modeling aspects; (1) dataset, (2) structural analysis model, (3) inter-subject and intra-subject variability (statistical) model, and (4) covariate models. The structural models generally describe the typical drug concentration versus time relationship of the population. They can include the systemic model (e.g. description of kinetics following intravenous dosing) and the absorption model (e.g. description of drug uptake in the blood for extravascular dosing). The inter-subject and intra-subject variability model detail the random variability in the population (e.g. residual, occasional and inter-subject). Covariate models detail the variability predicted by covariates of the individual study subjects. Non-linear mixed-effect modeling combines the models, applying an estimation method for the determination of the structural analysis model, inter-subject and intra-subject variability model, and covariate model parameters that describe the data. (Bonate 2011)

1.5.3 Statistical Modeling

The development of an appropriate inter-subject and intra-subject variability model is essential for proper evaluation of PK/PD data, as well as for simulation. In population PK models,

three inter-subject, and intra-subject variability (statistical) models are commonly used. (Lala , et al. 2012) The between-subject variability (BSV) or interindividual variability model indicates a random unexplained variance between subjects, while the between occasion variability (BOV) model describes individual variance between different occasions. Within-subject variability (WSV) or residual variability model describe unknown or unexplained variability despite controlling for known sources of variability. The WSV, also known as intra-individual variability, may represent model misspecification and error in the measurement of the assay. The parameters obtained from these inter-subject and intra-subject variability models quantify random, unknown variations. (Mould, et al. 2012, Burger, et al. 2014)

Between-Subject Variability (BSV)

It is unlikely that a parameter in a model will be constant across all individuals. It is presumed that all model parameters are random and that there will be some variation in the values across all individuals. However, such assumption is not realistic due to the fact that the right type of data has not been collected or not enough data has been compiled to estimate the variability of a particular parameter in a population and hence the model needs to be simplified by considering that particular parameter as a fixed effect. (Lacey, et al. 1997; Limpert, et al. 2001; Mould, et al. 2013) Consequently, it is logical to have a model with some fixed parameters across all individuals and some parameters with variability across individuals. In certain cases where the variability across individuals can be estimated, the choice of how to model the variability usually depends on the type of data. PK data is often modeled on an exponential scale because the parameters of PK models must be constrained to be greater than zero and are usually right-skewed. (Mould, et al. 2013.)

Between-Occasion Variability (BOV)

Individual PK parameters can vary with time, and the source of the variability is determined by the occasion. Initially, between-occasion variability (BOV) was defined as an residual unexplained variability component (RUV) (Karlsson, et al. 1993) and was later cited as a component of BSV. The BOV should be evaluated whenever appropriate. As reported by Karlsson and Sheiner, bias was observed to exist in both variance and structural parameters when BOV was completely ignored. (Karlsson, et al. 1993) However, the degree of bias depended on the design of the study, the magnitude of the BOV, and the inter-individual variability. Failure to consider BOV may result in an increased chance of statistically significant bias in the period of time in parameter estimates.

Within-Subject Variability

Within-subject variability (WSV), or RUV, arises from a variety of sources, such as as assay variability, incorrect sample time collection, dosing errors, and model misspecification. The WSV model selection usually depends on the type of data evaluated and is similar to the BSV model. (Mould, et al. 2013) The model that determines the within-subject variability is known as the residual variance model. The more heterogeneous and substantial the residual variance, the higher the need for it to be included in the overall model. WSV depends on specific covariates, such as changes in the assay between studies, variations in the execution of studies, or the involvement of different patient populations requiring different WSV models. (Mould, et al. 2002)

1.5.4 Covariate Model Analysis

One of the critical terms in population PK study is "covariate," which relates to any variable that is limited to an individual. Covariates are categorized into intrinsic factors such as those that

are genetically determined or inherited, or age, height, weight, and race; and extrinsic factors that are influenced by the external environment such as drug dose, degree of medication adherence, smoking habits, and presence of adjuvant medications. Covariates can be classified as continuous (e.g. age), dichotomous (e.g. sex), or polychotomous/categorical (e.g. race). Generally, intrinsic covariates do not differ over a short duration, whereas extrinsic covariates can differ during the course of a study. (Bonate, 2011) The covariate modeling method can be univariate or multivariate, and various methods for covariate selection have been described, including the classical stepwise covariate modeling method.

1.6 Pharmacodynamic (PD)

Pharmacodynamics (PD) is the study of the effect of drugs on the body. In other words, PD represents a drug effect at the physiological, biological, and molecular levels. (Benet, et al. 1995, Campbell, et al. 2017) The recognition of PD science began in the mid-1960s with the work of Dr. Gerhard Levy, who first described an association between drug concentrations and reversible drug reactions using mathematical equations. (Levy, et al. 1964, Levy, et al. 1966) Since then, PD modeling has emerged as a significant field to mathematically outline drug effects. (Mager, et al. 2003) PD modeling is now crucial for regulatory review of new therapeutics. (Huang, et al. 2013)

Different types of PD models range from linear models to more complex models. The relationship between plasma concentrations and PD response of a drug, whether beneficial or adverse, can be evaluated using simple direct effect models such as the liner pharmacodynamic model, Emax model, and sigmoidal Emax model. (Holford, 2017) In the Emax model, the drug effect is directly proportional to the drug concentration. The Emax model can be described as shown in Eq.4; where E is defined as the drug effect (observed), Emax is defined as the maximal

drug effect, Conc is defined as the drug concentration, and EC50 is defined as the concentrations that produce half of the maximal effect.

$$E = \left(\frac{E_{max} \text{ x } Conc}{EC_{50} + Conc}\right) \quad (4)$$

Note that Emax and EC50 can be denoted as Imax and IC50 for drugs that have inhibitory effects. At very low concentrations (below the EC50), the concentration-effect relationship became liner and can be described by the following equation (Eq.5)

$$E = Slope * Conecntration \quad (5)$$

When the concentration relationship's effect cannot be adequately fit with the Emax model, an extension of the Emax model introduces an additional exponent known as the Hill coefficient, called the sigmoidal Emax model. The Hill coefficient determines the 'steepness' of the effect versus concentration curve. Nevertheless, some drugs require time for their response due to an equilibration delay between the plasma compartment and the action site. This delay is seemingly not related to plasma concentrations but can be associated with the effect-compartment ('link') model. (Hull, et al. 1978; Stanski, et al. 1990)

Pharmacodynamic models can also be classified according to the time dependency, known as time-invariant and time-variant models. Time-invariant models are so named because the PD parameters remain constant over time. This model is sufficient for most drugs because their changes are directly related solely to their concentration at the effect site. However, with some drugs, the PD parameters can change as a result of tolerance (i.e., a decrease in the response) (Meibohm, et al. 2002) or sensitization (decrease in the number of receptors, or the receptor affinity) in the patient's system. (Ploeger, et al. 2009)

1.6.1 The Pharmacodynamic Modelling Concept

PD modeling can use a mechanism-based approach to offer insight into the mechanistic process behind drug effects. These semi-mechanistic response models are commonly sub-classified as indirect pharmacodynamic models, in which the effect of a drug indirectly related to secondary or a more intermediate response steps. (Agoram, et al. 2007; Danhof, et al. 2008) This classification can be dependent upon the pathophysiology of the disease state and requires an understanding and consideration of the mechanisms. Indirect response models are used to study the PD of a wide variety of drugs with an indirect mechanism of action. The first formal proposal of indirect response models was presented as four basic models by Dayneka and colleagues.(Dayneka, et al. 1993)

The basic structure of indirect models include inhibition of the production variable (k_{in}) (Model 1), inhibition of the dissipation variable (k_{out}) (Model 2), stimulation of the production variable (k_{in}) (Model 3), and stimulation of the dissipation variable (k_{out}) (Model 4), as presented in formed due to inhibition of the factors influencing the response variable kout dissipation. #3 represents Model 3, describes the drug response formed to stimulate the response variable kin development factors. #4 represents Model 4 describes the drug response produced due to stimulating the factors influencing the response variable kout dissipation.

(Jusko , et al. 1994, Sharma , et al. 1998)

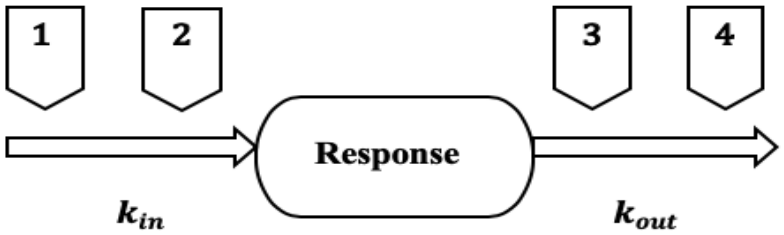

Figure 2. Structure of four basic indirect response models

Note #1 represents Model 1, outlines the drug response formed to inhibit the factors regulating the response variable kin's output; #2 represents Model 2, describes the drug response formed due to inhibition of the factors influencing the response variable kout dissipation. #3 represents Model 3, describes the drug response formed to stimulate the response variable kin development factors. #4 represents Model 4 describes the drug response produced due to stimulating the factors influencing the response variable kout dissipation.

Model 1 (Inhibition-k_{in})

Model 1 outlines the drug response formed as a consequence of inhibiting the factors regulating the output of the response variable k_{in}. Where I_{max} is the maximum fractional ability of the drug to influence the inhibition processes and IC_{50} is the drug concentration that produces half of the maximum inhibition. The I_{max} and IC_{50} inhibition mechanism are known to operate on a k_{in} as shown in Eq. 6:

$$\frac{dR}{dt} = k_{in}\left(1 - \frac{I_{max} \times C_p}{IC_{50} + C_P}\right) - k_{out} \times R \qquad (6)$$

(k_{in} is the zero-order rate constant. K_{out} is the first order rate constant. Imax is the maximum fractional ability of the drug to influence the inhibition processes. IC_{50} is the concentration that produces half of the maximum inhibition. The C_p value is the plasma drug concentrations).

Model 2 (Inhibition-k_{out})

Model 2 describes the drug response formed as a consequence of inhibition of the factors influencing the response variable k_{out} dissipation. Where IC_{50} is the concentration that produces half of the maximum inhibition. The mechanism of inhibition with an IC_{50} is considered to function on kout as shown in Eq.**Error! Reference source not found.Error! Reference source not found.** 7**Error! Reference source not found.Error! Reference source not found.** below:

$$\frac{dR}{dt} = k_{in} - k_{out}\left(1 - \frac{I_{max} \times C_p}{IC_{50} + C_P}\right)R \quad (7)$$

(I_{max} is the maximum fractional ability of the drug to influence the inhibition processes. IC_{50} is the concentration that produces half of the maximum inhibition. The C_p value is the plasma drug concentrations, R response).

Model 3 (Stimulation- k_{in})

Model 3 describes the drug response formed as a consequence of stimulating the factors regulating the response variable k_{in} development. The mechanism of stimulation process with SC_{50} is considered to function on the kin as shown in Eq. 8 below:

$$\frac{dR}{dt} = k_{in}\left(1 + \frac{S_{max} \times C_p}{SC_{50} + C_P}\right) - k_{out} \times R \quad (8)$$

(S_{max} is the maximum fractional capacity of the drug to affect stimulation. SC_{50} is the concentration which produces half of the maximum stimulation. Cp is the concentration of the plasma, R response)

Model 4 (Stimulation- k_{out})

Model 4 describes the drug response produced as a result of stimulating the factors influencing the response variable k_{out} dissipation. The mechanism of stimulation process with SC_{50} is considered to function on k_{out} as shown in Eq. 9 below:

$$\frac{dR}{dt} = k_{in} - k_{out}\left(1 + \frac{S_{max} \times C_p}{SC_{50} + C_P}\right)R \quad (9)$$

(S_{max} is the maximum fractional capacity of the drug to affect stimulation. SC_{50} is the concentration which produces half of the maximum stimulation. Cp is the concentration of the plasma, R response).

1.7 Summary

In summary, The sensitivity to drug-induced QT prolongation is highly variable in heart failure (HF) patients. QT interval prolongation can lead to a life-threatening ventricular arrhythmia known as torsade de pointes (TdP), resulting in sudden cardiac death. Although QT prolongation is a surrogate marker for sudden cardiac death, the extent of drug-induced QT prolongation, and thus TdP, is mostly unpredictable. Our research group has identified miR-362-3p as a potential regulator of the QT interval. Understanding the interplay between drug-induced QT interval lengthening in HF, in addition to serum miR expressioncould be enhanced through PK-PD models to assess circulating serum-miR as a potential biomarker for drug-induced QT-interval prolongation. Thus, the primary objective is to develop a semi-mechanistic model using the nonlinear mixed-effects approach to describe serum miR-362-3p expressions in the circulation as a potential biomarker to predict subject susceptibility to drug induced-QT interval prolongation. We hypothesize that subjects with higher serum miR-362-3 expressions are more susceptible to drug-induced QT interval prolongation.

1.8 Project Objective:

The primary objective was to develop a semi-mechanistic model to describe serum miR-362-3p expressions as a potential biomarker to predict sensitivity to ibutilide induced-QT interval prolongation in patients with HF.

CHAPTER 2. METHODS

The dataset utilized for the development of the population PK-PD model was acquired from a previously published clinical trial by our research group (Tisdale, et al. 2020). This study was originally designed as a prospective, single, parallel comparative study to determine the impact of heart failure with preserved ejection fraction (HFpEF) on sensitivity to drug-induced QT prolongation.

2.1 Ethical Aspect

The study was approved by the Indiana University Purdue University Indianapolis (IUPUI) Institutional Review Board (IRB). All patients provided written informed consent.

2.2 Study Subjects

Subjects were enrolled into one of the three study groups (1) heart failure with reduced ejection fraction (HFrEF), (2) HFpEF, and (3) Control group without documented HF that was matched to the HFpEF group by age and sex. Subjects enrolled in the HFpEF group met the following criteria: symptomatic HF, left ventricular ejection fraction (LVEF) ≥50% within the previous 2 years, and 1 or more of the following findings on the echocardiogram: E/E'> 15; E/A < 0.5; maximum left atrial volume index of >40 mL/m^2; and diastolic dysfunction grade 2 or greater.

2.3 Eligibility Criteria

In order to qualify for the study, subjects had to weigh between 60 and 130 kg. Serum magnesium concentrations were required to be higher than 1.8 mg/dL, and serum potassium concentrations greater than 3.8 mEq/L. Qualified subjects had hepatic transaminases less than

three times the standard upper limit, hematocrit above 26%, and estimated creatinine clearances of at least 20 mL/minute. Subjects were excluded from the study if they were pregnant or lactating, had an individual or family history of TdP, long QT syndrome, sudden cardiac death (not associated with myocardial infarction), or had New York Heart Association (NYHA) defined class IV heart failure. Subjects were also excluded for permanently paced ventricular rhythm or sustained arrhythmias, including atrial fibrillation. Patients who had been given Vaughan Williams Class 1a drugs or class III antiarrhythmic drugs within five half-lives of ibutilide infusion,had a baseline QTc interval above 450 ms, or had adjuvant use of QT interval-prolonging drugs were also excluded.

2.4 Study Design

The design included two phases (1) a study day dedicated to a screening phase and (2) a study day dedicated to the treatment phase. During the screening phase, enrolled subjects remained for 12 hours at the Indiana Clinical Research Center (ICRC) for baseline QT measures. Twelve lead ECGs (Marquette Mac 5500, GE. Healthcare Biosciences, Pittsburgh, Pennsylvania) were serially collected in triplicate (approximately 1 minute apart) at the following pre-specified time points; 0, 15, 30, and 45 minutes, and 1, 2, 4, 6, 8 and 12 hours. In the treatment phase, subjects received a single IV dose of ibutilide (0.03 mg/kg) diluted in 50 ml of normal saline and administered slowly via infusion pump over 10 minutes at the ICRC. Following IV infusion, triplicate 12 lead ECG readings and venous blood samples (10 mL) were collected at baseline from all the subjects and at the following pre-specified times; end of infusion and at 5, 10, 15, 20, 30, and 45 minutes, and 1, 2, 4, 6, 8, and 12 hours post-infusion. Blood (10 mL) samples were obtained using an indwelling catheter in the arm contralateral to that of the ibutilide infusion.

2.5 QT Interval Measurements and QT Interval Correction

Triplicate 12-lead ECGs were collected during both phases of this trial. The RR and QT intervals were measured from leads II, V1, and V5 using electronic calipers in the the MUSE automated system (GE. Healthcare Biosciences, Pittsburgh, PA). The triplicate ECG readings were collected approximately 1 minute intervals from pre-specified time points: at 0 minutes, at the end of infusion, at 5, 10,15, 20, 30, and 45 minutes, and later on at 1, 2, 4, 6, 8 and 12 hours. The QT intervals were corrected for heart rate using the Fridericia formula.

2.6 Serum Ibutilide Concentration Assay

The serum was separated from whole blood and then stored (-70° F) until further analysis. Serum ibutilide concentrations were determined in the Indiana University Clinical Pharmacology Analytical Core (CPAC) Laboratory using reverse-phase high-performance liquid chromatography with mass spectrometry (HPLC-MS) detection (Agilent 1290 HPLC, Eksiegent Autosampler, and AB Sciex 5500 MS).

2.7 Quantitative Reverse Transcriptase-Polymerase Chain Reaction (q-PCR) Analysis

A total of 500 ng RNA of each sample was reverse transcribed using the High Capacity RNA-to-cDNA Kit (Applied Biosystems, Foster City, CA, USA). According to the manufacturer's recommendation, the extracted RNA synthesized the cDNA by mixing the RNA with reverse transcriptase enzyme mix, random sequence oligonucleotide, and nuclease-free water and using the TaqMan Gene Expression Assays kit (Life Technology, Carlsbad, CA, USA).

2.8 Population Pharmacokinetic-Pharmacodynamic Analysis

2.8.1 Software

Pharmacokinetic/Pharmacodynamic modeling was performed using a nonlinear mixed-effect model approach (NONMEM, Version 7, ICON Development Solutions, Ellicott City, MD, USA). The population parameters were evaluated using the classical first-order conditional estimation method with interaction (FOCE-I). (Bauer 2019) The adjunct tools used to evaluate the population PK-PD model utilized during the modeling process were R (version 3.1.2) and XPose (version 4.5.3), along with the graphical interface Pirana version 2.9.0. (Lindbom, et al. 2005, Keizer,et al. 2013)

2.8.2 Structural PK Model

Initially, a non-compartmental analysis (NCA) was performed to determine the preliminary pharmacokinetic input parameter estimates utilized during the population PK modeling process. Briefly, the total area under the concentrations-time curve (AUC 0-∞) was calculated using the trapezoidal rule. Clearance (CL) was estimated by dividing the ibutilide dose over the total area under the concentrations-time curve (AUC 0-∞). The volume of distribution (V) was calculated by multiplying the clearance (CL) by the mean residence time (MRT), and finally, the terminal half-life (t1/2) was calculated by dividing 0.693 over the slope of the terminal phase (ke).

Summary of NAC

Parameters	Median
AUC0--∞ (mg*hr/mL)	2.5
CL (mL/hr/kg)	0.10
V (mL/kg)	0.01
t1/2 (hr)	6.04
Ke (1/hr)	0.044

Several structural population PK models were investigated (e.g. two compartments and three-compartment models). Multiple criteria were used to determine the selection of the final population PK base model including; likelihood ratio test, visual inspection of the goodness-of-fit (GOF) plots, precision in parameter estimates, the Akaike information criterion (AIC), and consistency with previously published ibutilide PK-PD parameters. (Tisdale, et al. 2008, Zeng, et al. 2017)

2.8.3 Structural PK-PD Model

The PD response model was developed using an indirect response model based on its mechanistic effects (I_{Kr} inhibition) with zero-order input parameter and output parameter predicting the QT interval prolongation. The selected PD model provided the best fit to the observed data as described in equation

$$\frac{dQT}{dt} = Kin * EFF(CON) - Kout * dQT$$

$$EFF(CON) = 1 - \left(\frac{Imax * Conc}{IC50 + Conc}\right) \quad (11)$$

Where Kin denotes the zero-order rate constant, and Kout denotes the first-order rate constant; EFF(CON) is the effect of ibutilide concentrations on QT. Imax denotes the maximum effect, and IC50 denotes the ibutilide-plasma concentration that is required to achieve 50% of the maximum effect on QT.

Baseline QTc from both phases was included as the dependent variable. To account for diurnal variation associated with baseline QT interval, an inter-occasion term on the QT baseline parameter was utilized according to the following equation:

CC=0, IF (TIME.GT.12) =OCC1

IOV(1-OCC) *ETA (5) +OCC*ETA (6)

OMEGA BLOCK (1) 0.05; IOV VARIANCE OMEGA BLOCK (1) SAME

where IOV are random variables between occasion IOVs and OCC denotes each phase, with OCC0 representing the screening phase (day 1) and OCC1 representing the ibutilide phase (day 2).

2.7.4 Covariate Analysis

A structural base model was used to determine all the possible contributions of pre-specified covariates contribution to the observed variability in the PK model of ibutilide and ibutilide-induced QT-interval (PK-PD model). The selection of covariates was initially based on the forward addition technique in which covariates are added to the base model, and then the backward elimination was utilized to remove one at a time. Covariates were considered statistically significant if the objective function value (OFV) decreased by > 3.84 units after the addition of each covariate. Similarly, only covariates that increased the OFV by > 6.63 units during backward elimination were kept in the model.

For continuous covariates, the following functional forms were utilized:

a. Linear

$$TV\theta = \theta + \theta_{cov} * (COV - COV_{median}) \quad (12)$$

NONMEM coding

$$TV\theta = THETA(1) * THETA(2) * (COV - COV_{median}) \quad (13)$$

$$\theta = TV\theta * EXP\big(ETA(1)\big)$$

b. Power

$$TV\theta = \theta * (\frac{COV}{COV_{median}})^{\theta cov} \quad (14)$$

NONMEM coding

$$TC\theta = THETA(1) * \left(\frac{COV}{COV_{median}}\right) ** THETA(2) \quad (15)$$

$$\theta = TV\theta * EXP\big(ETA(1)\big)$$

c. Exponential

$$TV\theta = \theta * EXP(\theta_{cov} * (COV - COV_{median})) \quad (16)$$

NONMEM coding

$$TV\theta = THETA(1) * EXP(THETA(2) * (COV - COV_{median})) \quad (17)$$

$$\theta = TV\theta * EXP\big(ETA(1)\big)$$

(TVθ reflects the population value of the parameter for a given covariate value and θ is the population value of the parameter for those individuals with a covariate value equal to the median value (COV_{median}) as for those individuals $COV-COV_{median}= 0$ or $COV / COV_{median}= 1$. θ_{cov} reflects a fractional change in population parameter value due to the covariate effect).

In NONMEM equations, TVθ is a standard value parameter with a covariate median value (COV_{median}). θ is the parameter estimate; ETA (1) is the parameter estimate difference between the person and the population. THETA (2) is a factor that describes covariate influence (COV).

2.8.4 Random Effect Model

The inter-individual variability of the PK and PD model parameters for each patient was best described by an exponential model (Equation **Error! Reference source not found.**) as shown below (Feng, et al. 2006):

$$Pi = \theta * \exp(\eta p) \quad (18)$$

Where Pi is the individual parameter estimate for the subject; θ is the population mean estimate for parameter P; and (ηp) denotes the difference between Pi and θ.

The intra-individual variability (residual error model, RUV) was best described by proportional error for the PK model and by additive error for the PD model. The proportional error equation (19) is presented below (Choi, et al. 2016):

$$DV = IPRED + (IPRED * \varepsilon 1) \quad (3)$$

Where DV is the dependent variable for the observed PK/PD model, IPRED is the PK, and PKPD model-predicted concentrations/effect for the individual and ε1 and ε2 are the differences between the individual observed and individual predicted concentrations/effect.

2.9 Model Evaluation

The criteria for model evaluation included objective function value (OFV), Akaike information criterion (AIC), visual assessment of the goodness of fit plots (e.g., predicted versus observed concentrations; weighted residual versus predicted concentration), and overall plausibility and precision of the PK and PK-PD parameter estimates. Furthermore, a drop-in OFF

of > 3.84 ($p < 0.05$, degrees of freedom = 1) was considered a significant decrease in the objective of the function value. The visual predictive check (VPC) was performed to further confirm the accuracy and predictive performance of both the PK and PK-PD output using the final parameter estimates to simulate a profile of 1,000 individuals by prediction of the 95 percentiles. The median and the fifth and ninety-fifth percentiles were determined and then superimposed with the original data. The model was considered to appropriately represent the data if most of the observed data points fell within the fifth and 95 percentile intervals and were equally distributed around the median. (Baheti et al. 2011, Park, et al. 2014)

CHAPTER 3. RESULTS

3.1 Clinical and Demographic Characteristics of all Subjects

A total of 22 subjects (15 women and 7 men), aged 18 to 80 years who met the inclusion and exclusion criteria were enrolled and divided into three groups: a group of heart failure with preserved ejection fraction (HFpEF, n=10), a group of heart failure with reduced ejection fraction (HFrEF, n=2), and ten healthy subjects in the control group were matched to subjects in the HFpEF for age (67±10 years) and sex. There were no significant differences in terms of age and weight in all groups. Overall, a total of 536 ibutilide serum concentrations, serum miR-362-3p expressions, and QT interval data points were included in the analyses. **Error! Not a valid bookmark self-reference.** shows the demographics and clinical characteristics of study subjects.

Table 1. Participant Demographics and Subject Characteristics

Characteristic	**Matched Controls (n=10)**	**HFpEF (n=10)**	**HFrEF (n=2)**
Male sex, n (%)	3 (30)	3 (30)	1 (50)
White, n (%)	8 (80)	7 (70)	1 (50)
African American, n (%)	2 (20)	3 (30)	1 (50)
Age, years	67 ± 9	69 ± 8	67 ± 1
Weight, Kg	82.2 ± 12	89.7 ± 13	87.3 ± 3
Ibutilide dose, mg	0.25 ± 0.04	0.27± 0.04	0.26 ± 0.01
Serum miR-362-3p, n (%)	2 (20)	8 (80)	2 (100)
Concurrent diseases, n (%)			
- Hypertension	6 (60)	8 (80)	2 (100)
- Coronary artery disease	1 (10)	3 (30)	2 (100)
- Diabetes mellitus	2 (20)	5 (50)	1 (50)
- Hyperlipidemia	6 (60)	5 (50)	2 (100)
Concomitant medications, n (%)			
- ACE inhibitors/ARBs	3 (30)	7 (70)	2 (100)
- Loop diuretics	2 (20)	7 (70)	2 (100)
- Beta-blockers	2 (20)	8 (80)	2 (100)
- Statins	4 (40)	5 (50)	2 (100)

Note: **HFpEF** = Heart failure with preserved ejection fraction; **HFrEF**= Heart failure with reduced ejection fraction; Data presented as n (%) or mean ± S.D.

3.2 Population PK Modeling

The population PK model was developed to describe ibutilide serum concentration versus time. The PK model was estimated using the first-order conditional estimation method with an interaction term (FOCE-I). The PK parameters of ibutilide were evaluated by both two- and three-compartment PK models (implemented via ADVAN3, TRNAS4, ADVAN11, and TRANS4 subroutines receptively) with first-order elimination from the central compartment. The final population PK base model was selected based on the objective function value (OBJ), Akaike information criterion (AIC), visual inspection of the goodness of fits plots, individual and population parameter estimates, and reduction in both residual and interindividual variability.

Following noncompartmental analyses, a 2-compartment model with first-order elimination from the central compartment was compared to a 3-compartment model. The two compartmental models' apparent volume of distributions parameter was poorly estimated, reflected by a large shrinkage value greater than 30%. The term shrinkage refers to the residual error in the model calculated as 1-SD (individual weighted residuals). Therefore, for larger shrinkage value; the individual predictions shrink back toward the observation where theDV is equal to the IPRED. The goodness of fit plots (GOF) for the 2 compartment model are presented in Figure 3 along with model evaluation criteria with the parameter estimates listed in Table 2. In addition to improving the model fit, the PK parameter estimates from the three compartment model aligned with those previously reported. Accordingly, the structural population PK model was best described by a 3-compartment model with first-order elimination from the central compartment, as illustrated in Figure 4. While other residual error models did not significantly improve the model fit (delta OFV < 3.84) as shown by the GOF in Figure 5, A proportional error model best described the residual variability. The mean parametervalue of ibutilide clearance (CL) was 199 L/hr, the mean volume distribution of the central compartment (VC) was 28.6 L; and the mean volume distribution of

peripheral compartment 1 (VP1) and f peripheral compartment 2 (VP2) were 80.2 L and 1020 L, respectively.

3.3 Covariate Analysis—PK Model

In analyzing the covariate relationships, each covariate was added univariately in the base model using centered, linear, exponential, or power relationships, as presented in Table 3.. The tested covariates did not have a significant effect on any of the PK parameters. Hence, the base structural model represented the final PK model.

3.4 Model Evaluation

The dependent variable (observed ibutilide serum concentration) vs Individual predicted serum concentration (IPRED) vs time along with the GOF plots indicated no misspecifications in the model (Figures 5 & 6). The predictive performance was determined to be acceptable, as most of the observed data points contained in the model's 90% confidence interval of the predictions reflect the 5th–95th percentiles as displayed in Figure 7. The final population PK parameter estimates for both the fixed-effect and random-effect parameters were in close agreement with the corresponding median estimates derived from the bootstrap, as displayed in Table 4.

Table 2. A 2-Compartmental Population PK Model Parameter Estimate for Ibutilide

Parameter	Population Estimates (RSE %)
CL, L/hr.	264 (7%)
Q, L/hr.	566 (12%)
V_c, L	62.5 (12%)
Vp, L	940 (7%)
ω Cl	0.104 (52%)
ω Q	0.0633 (43%)
ω Vc	0.015 (39%)
ω V_p	0.109 (100%)
σ PROP	0.0611 (14 %)

Note. CL = systemic clearance, **Q**= Intercompartmental clearance, **Vc** = Volume distribution of central compartment, **Vp** = Volume distribution of peripheral compartment, **ω** = Inter-individual variability (omega), **σ** = Residual variability (sigma), **PROP** = Proportional, **RSE** = Residual standard error.

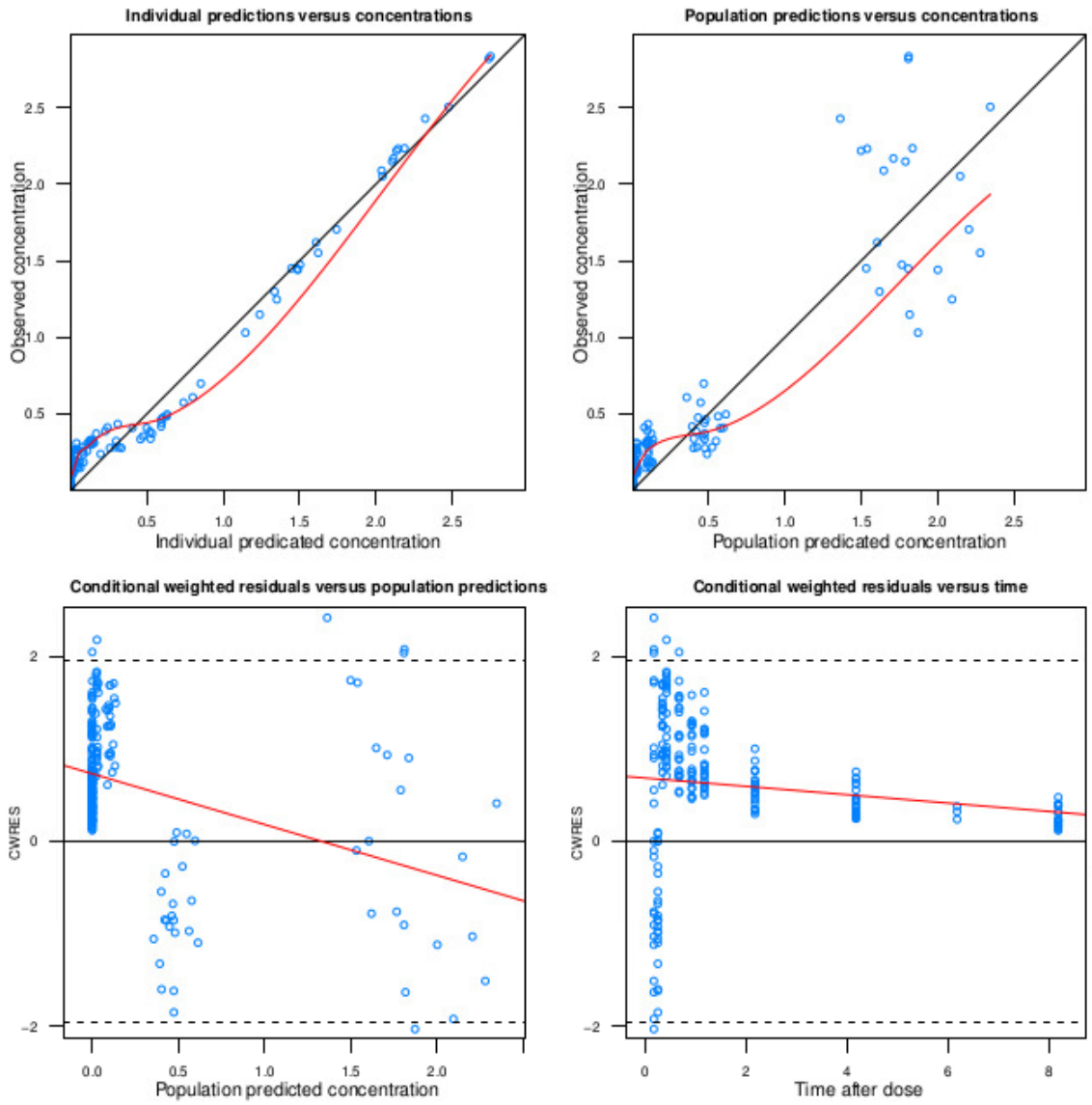

Figure 3. Goodness-of-fit plots for the 2-compartmental population PK model of ibutilide

Note. **(A)** observed ibutilide concentrations vs. individual predicted ibutilide serum concentrations **(B)** observed concentrations vs. population predicted concentrations **(C)** Conditional weighted residuals versus population predicted concentrations **(D)** Conditional weighted residuals versus time.

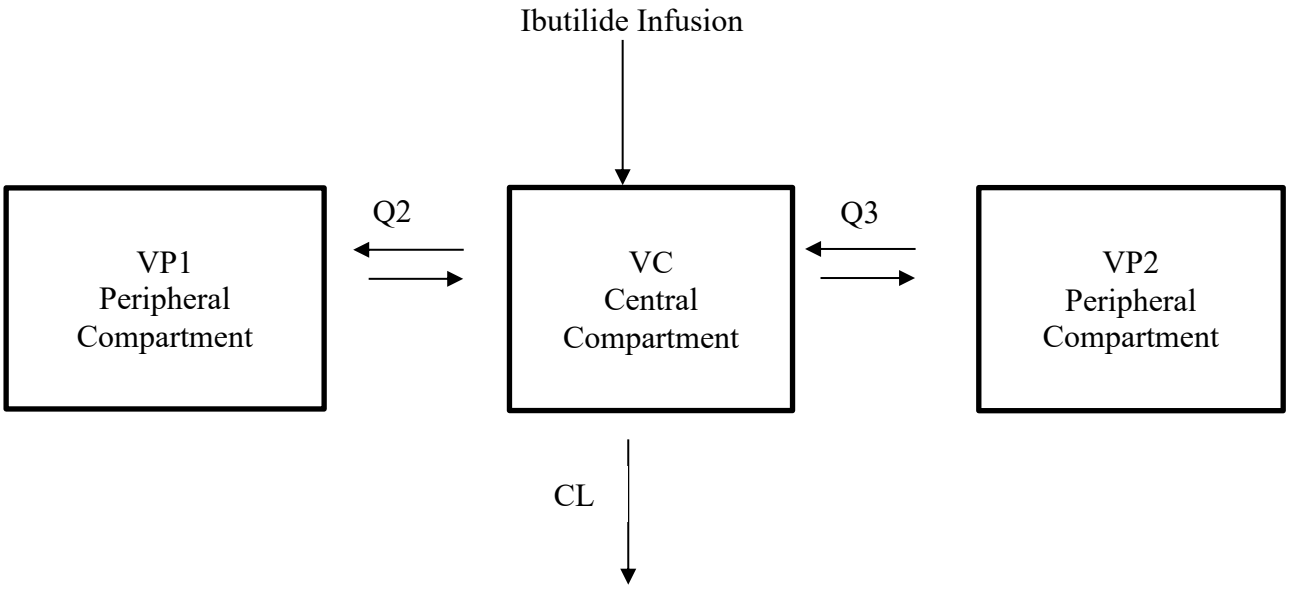

Figure 4. Display the Three Compartmental Structural Pharmacokinetic Model of Ibutilide

Note. **CL** = systemic clearance, **Q2** = Intercompartmental clearance 1, **Q3**= Intercompartmental clearance 2, **Vc** = Volume distribution of central compartment, **Vp1** = Volume distribution of peripheral compartment 1, **Vp2** = Volume distribution of peripheral compartment 2.

Table 3. Summary of Pop-PK Model Covariate Analysis

Model Parameter	Covariate	OBJ	Δ OBJ	P-value	Functional Form
CL	Weight	-1280.914	0	NS	Power
CL	Weight	-1280.914	0	NS	Additive
CL	Weight	-1280.914	0	NS	Exponential
Vc	Weight	-1280.914	0	NS	Power
Vc	Weight	-1280.914	0	NS	Additive
Vp1	Weight	-1280.914	0	NS	Power
Vp1	Weight	-1280.914	0	NS	Additive
Vp1	Weight	-1280.914	0	NS	Exponential
Vp2	Weight	-1280.914	0	NS	Power
Vp2	Weight	-1280.914	0	NS	Additive
Vp2	Weight	-1280.914	0	NS	Exponential
CL	AGE	-1280.914	0	NS	Power
CL	SEX	-1280.914	0	NS	Power
CL	RACE	-1280.914	0	NS	Power

Note. **OBJ** = The objective function value; Δ **OBJ** =the difference in objective function values between the base and the added covariate model', **Vc**= Systemic clearance from the central compartment**; Vc**= Volume distribution of central compartment, **Vp1**= Volume distribution of peripheral compartment 1, **Vp2**= Volume distribution of peripheral compartment 2; **WT** = Weight; **NS**= Non-significant.

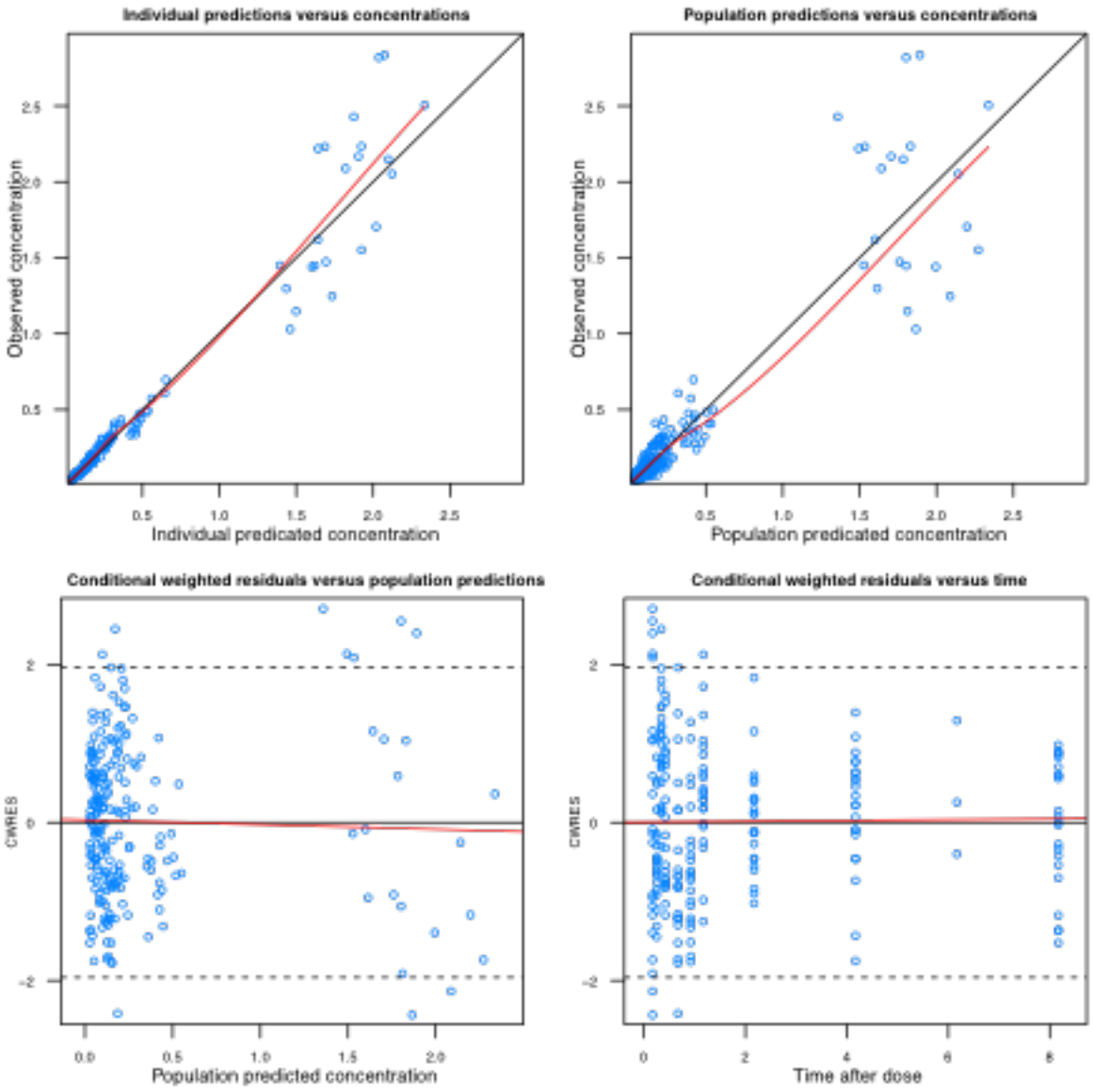

Figure 5. Goodness-of-fit plots for the final population PK model of ibutilide

Note. **(A)** observed concentration vs. Individual predicted concentration. **(B)** observed concentration vs. Population predicted concentration. **(C)** Conditional weighted residuals versus Population predicted concentration. **(D)** Conditional weighted residuals versus time.

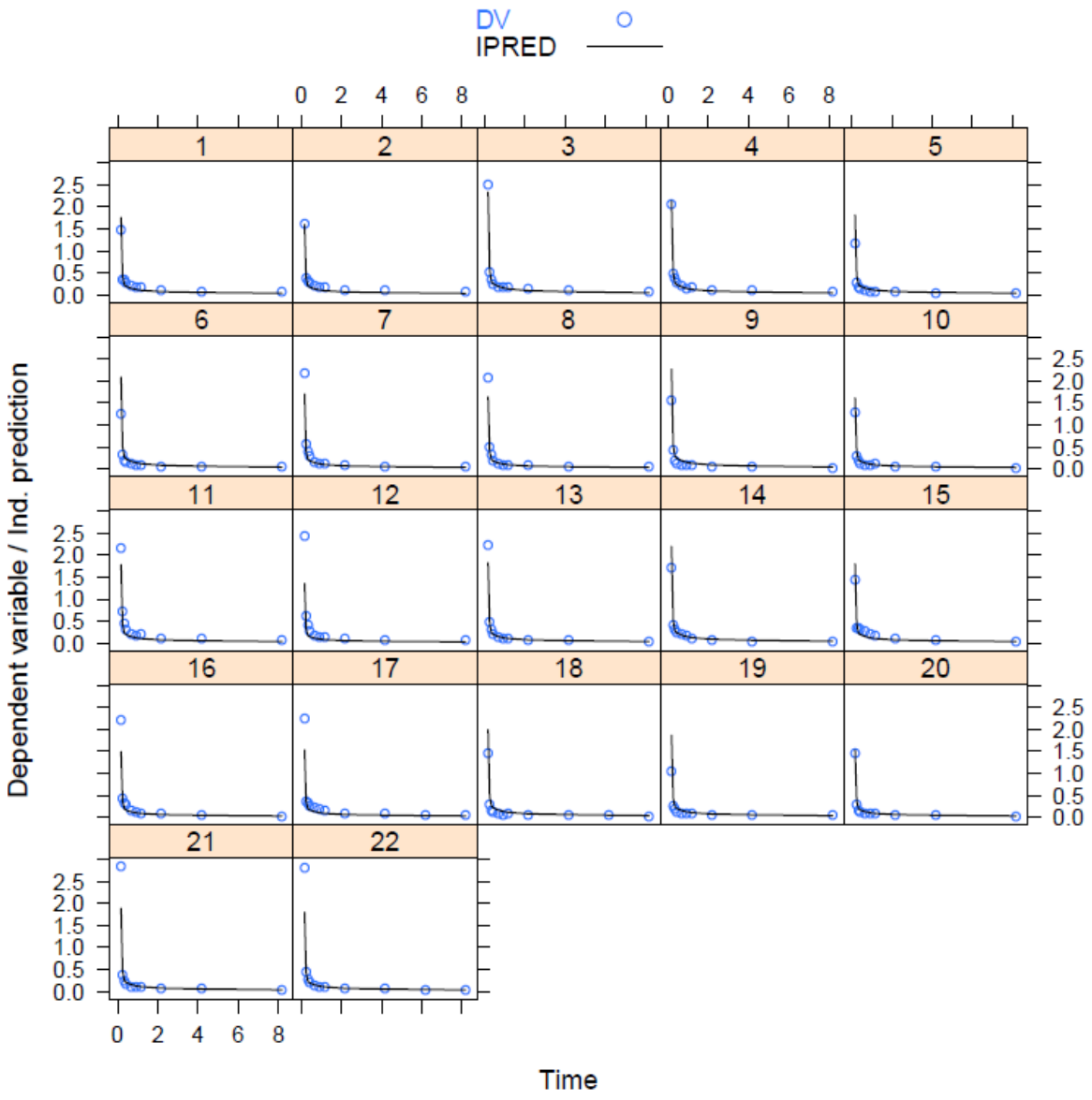

Figure 6. Individual plots for the final PK model outputs

Note. Open circles are observed ibutilide serum concentrations. Solid lines are individual predicted ibutilide serum concentrations.

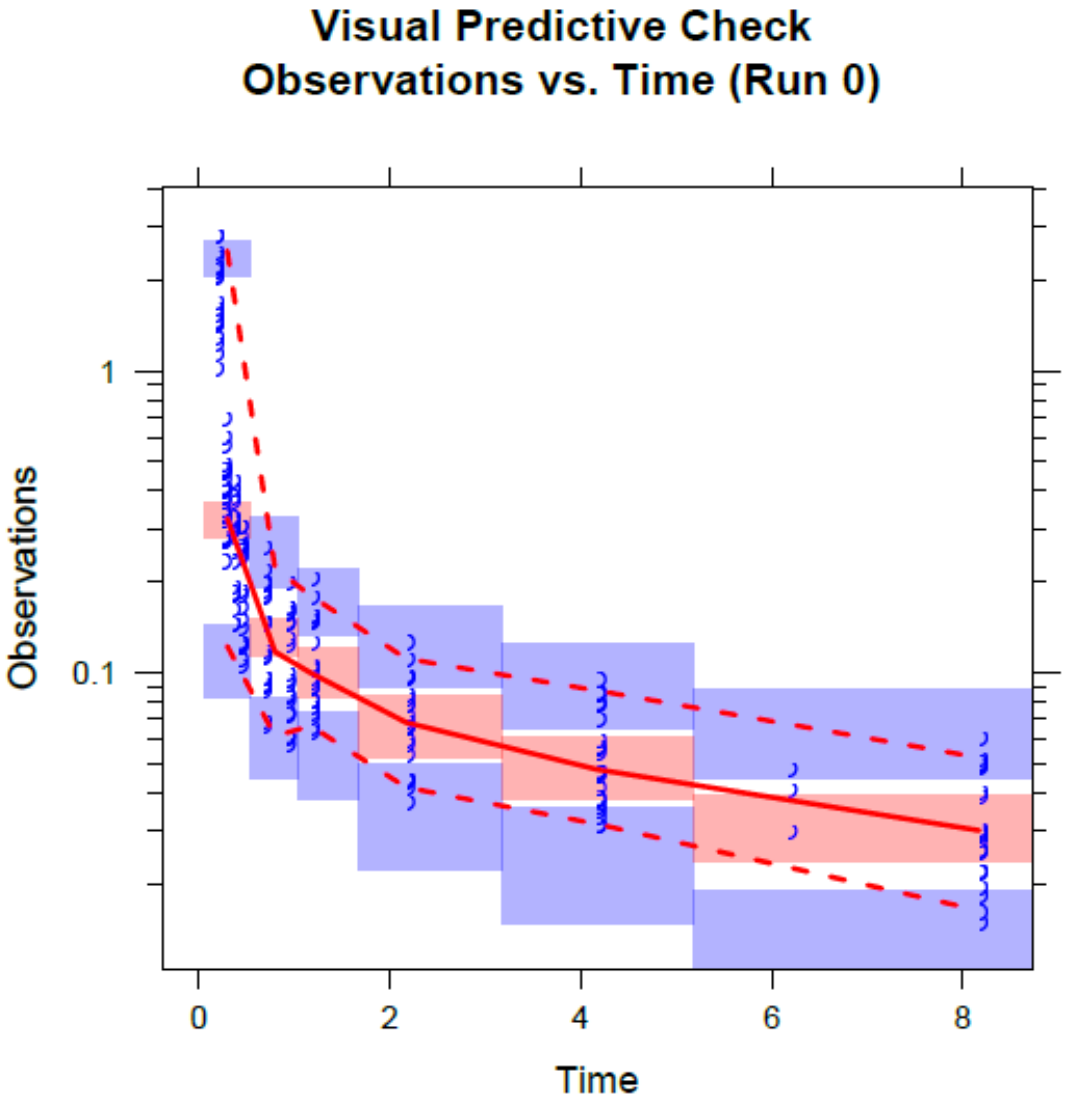

Figure 7. Visual predictive checks (VPC) of the final pharmacokinetic model

Note. Ibutilide serum concentrations(ng/mL) are represented by open. The observed 5% and 95% percentiles are presented with dashed red lines, and the 95% confidence intervals for the corresponding model predicted percentiles as described by semitransparent blue fields.

Table 4. Final Population Pharmacokinetic Model and the Bootstrap Median Parameter Estimate for Ibutilide

Parameter	Population Estimates (RSE%)	Bootstrap Median (95 CI%) *
Cl, L/hr.	199 (8.7%)	203.18 (165.09 - 232.90)
Cl_{ic1}, L/hr.	209 (8.1%)	207.92 (175.87 - 242.12)
Cl_{ic2}, L/hr.	316 (5.5%)	327.01 (281.70 - 350.30)
V_c, L	28.6 (7.9%)	29.86 (24.19 - 33.01)
V_{p1}, L	80.2 (0%)	80.20 (80.20 - 80.20)
V_{p2}, L	1020 (7.9%)	1075.58 (862.41 - 1177.58)
ω Cl	0.103 (30.8%)	0.109 (0.0514 – 0.175)
ω Cl_{ic1}	0.055 (45%)	0.057 (0.0136 – 0.104)
ω Cl_{ic2}	0.039 (34.1%)	0.036 (0.0134 – 0.0649)
ω Vc	0.01 FIX	-
ω V_{p1}	0.01 FIX	-
ω V_{p2}	0.146 (36.8%)	0.116 (0.0255 – 0.204)
σ PROP	0.026 (11.2 %)	0.0255 (0.02 – 0.0316)

Note. **Cl_s** = systemic clearance, **Cl_{ic1}** = Intercompartmental clearance 1**,** **Cl_{ic1}** = Intercompartmental clearance 2, **Vc** = Volume distribution of central compartment, **Vp_1** = Volume distribution of peripheral compartment 1, **Vp_2** = Volume distribution of peripheral compartment 2, **ω** = Inter-individual variability (omega), **σ** = Residual variability (sigma), **PROP** = Proportional, **RSE** = Residual standard error, **CI** = Confidence interval.

3.5 Population PK-PD Model

For the PD model, 444 QT intervals recorded from all subjects were included as the dependent variable. The relationship of ibutilide serum concentration versus time profile and its effects to induce QT interval prolongation were assessed. Individual ibutilide serum concentration versus time profiles were included with an indirect response model where ibutilide serum concentrations were indirectly driving QT interval prolongation through inhibition of the output (Kout) parameter. The indirect PK-PD model is schematically illustrated in Figure 8. A

high inter-occasion variability due to day-to-day variability in the QT baseline was observed. Thus, an inter-occasion terms was estimated on the baseline QT parameter. The addition of IOV resulted in a significant reduction of inter-occasion variability (OBJ decreased by a value of 69). Hence the addition of the IOV term improved the model fit to the data. The visual inspections of the GOF plots for the structural PK-PD model are displayed in Figures 9 & 10. The objective function values and the Akaike Information Criterion (AIC) were evaluated. The structural parameters estimated from the indirect PK-PD model were for the Imax and IC_{50} 0.115 ms and 0.36 ng/mL, respectively. Table 5 shows the parameter estimates and bootstrap analysis of the structural PK-PD parameters.

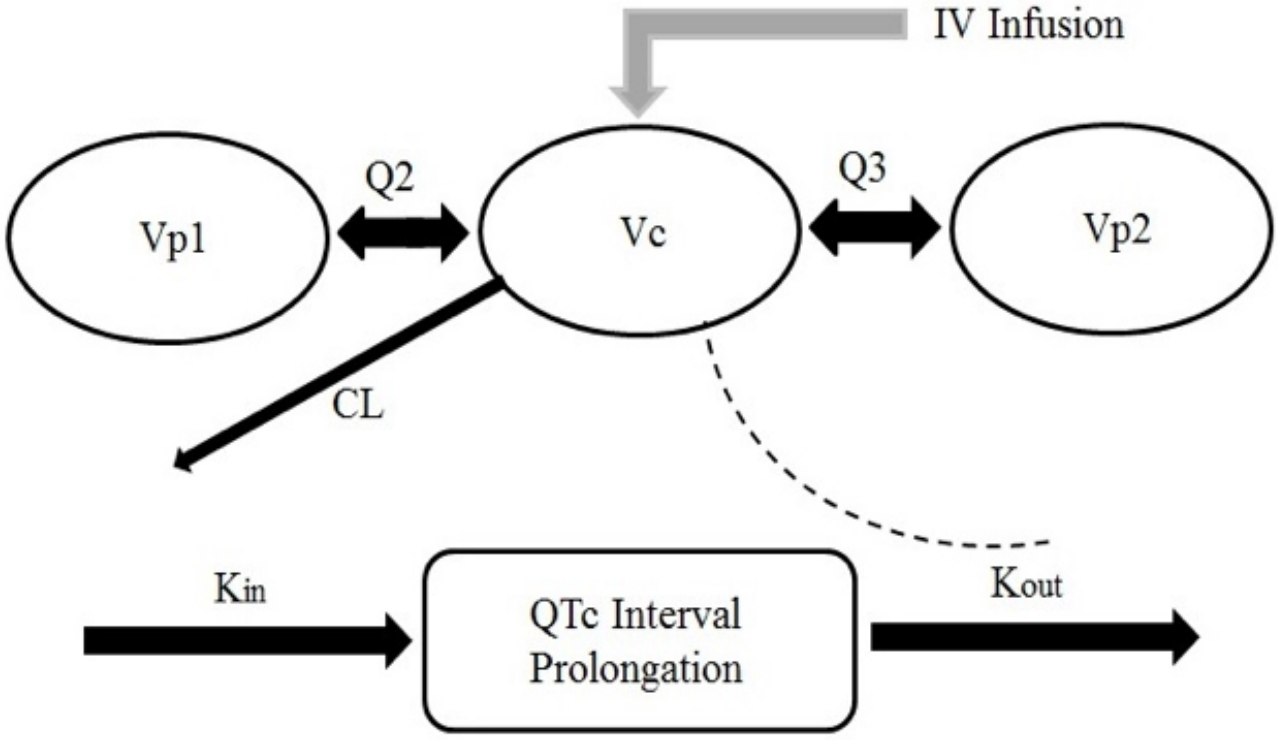

Figure 8. Schematic Representations of Ibutilide PKPD Model Indirect Effect

Where CL = systemic clearance, VC = volume distribution of the central compartment, VP1 = volume distribution of peripheral compartment 1, VP2 = volume distribution of peripheral compartment 2, Q2 = intercompartment clearance for compartment 2, Q3 = intercompartment clearance for compartment, Kin denotes the zero-order rate constant, and Kout denotes the first-order rate constant; EFF(CON) is the effect of ibutilide concentrations on QT. Imax denotes the maximum effect, and IC50 denotes the ibutilide-plasma concentration that is required to achieve 50% of the maximum effect on QT.

$$\frac{dQT}{dt} = Kin * EFF(CON) - Kout * dQT$$

$$EFF(CON) = 1 - \left(\frac{Imax * Conc}{IC50 + Conc}\right)$$

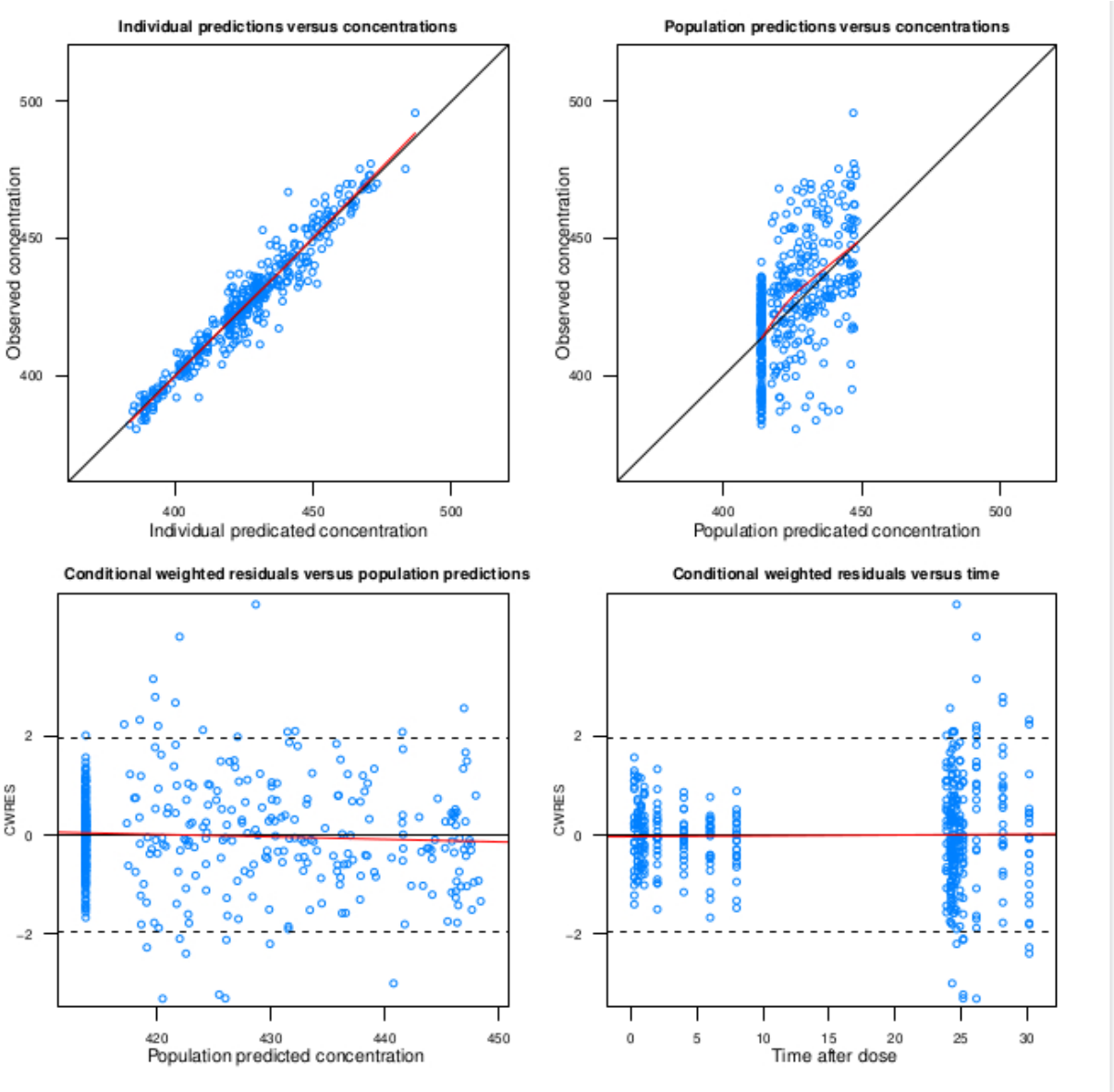

Figure 9. The goodness-of-fit plot of the structural pharmacokinetic-pharmacodynamic model of ibutilide

Note. (**A**) Observed QTF interval versus individual predicted QTF interval (ms) (**B**) observed QTF interval versus Population predicted. (**C**) Conditional weighted residuals versus Population predicted concentration. (**D**) Conditional weighted residuals versus time.

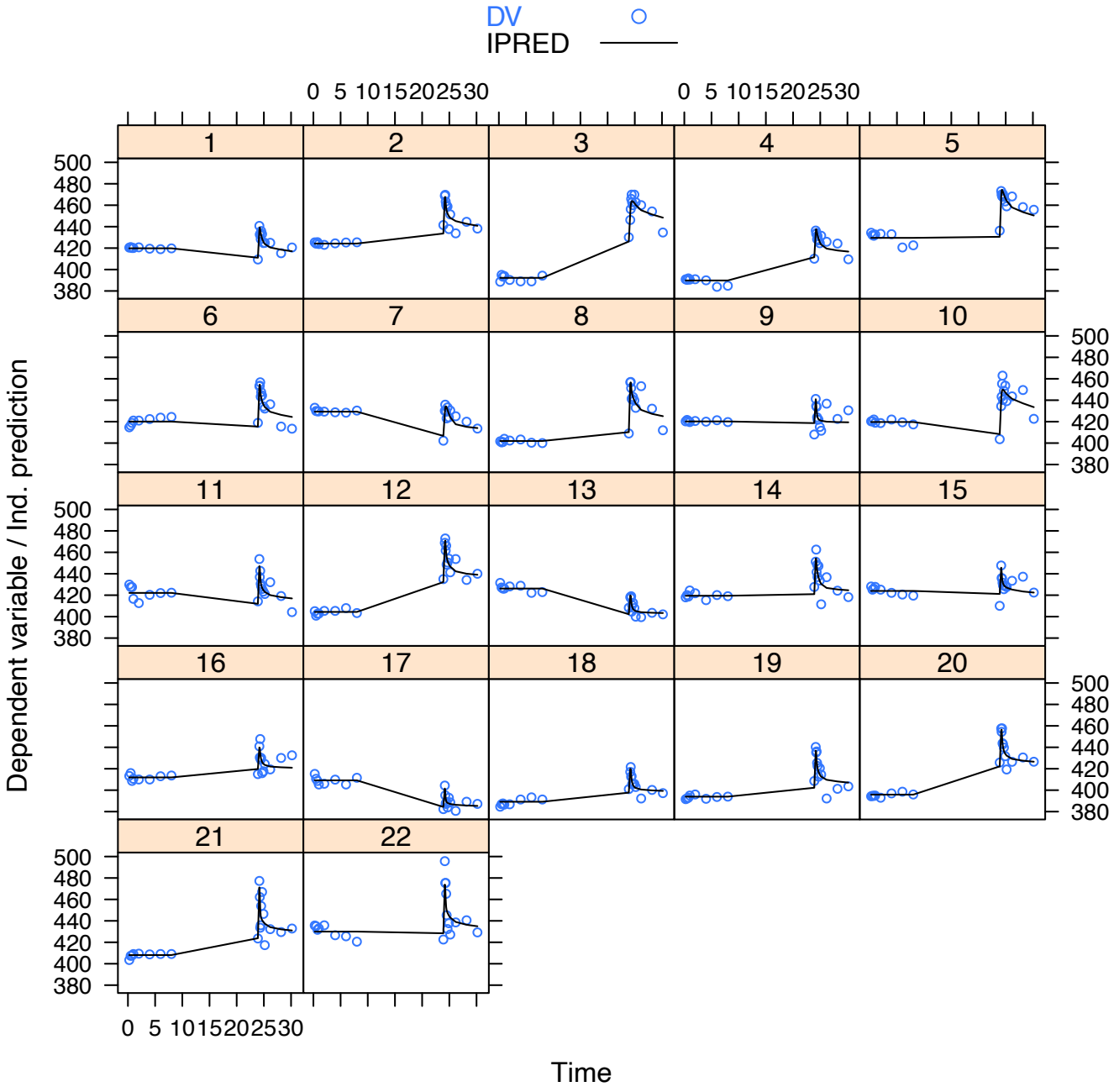

Figure 10. Individual plots for final PK-PD model outputs.

Note. Open circles are observed QT interval. Solid lines are individual predicted ibutilide serum concentrations.

Table 5. Summary of Estimated Population PKPD Parameters from the Base Model

Parameter	Population Estimates (RES%)	Bootstrap Median (95 CI%) *
I_{max} (%)	11.4% (9.9)	(0.088 – 0.142)
IC_{50} (ng/mL)	0.36 (8.4%)	(0.301 - 0.419)
Baseline QT (ms)	414 (0.5%)	(409.59 - 418.41)
K_{out} (hr^{-1})	9.75 (3.4%)	(9.005 - 10.295)
ω K_{out}	0.35 (31.2%)	-
ω IC_{50}	1.56 (9%)	-
ω Base QT	0 FIX	-
IOV Variance	0.0009 (5.8%)	-
IOV Variance	0.0009 (14.2%)	-
σ PROP	0.0002 (8.7%)	-

Note. * Based on Percentiles. **Base**= pre-ibutilide dose QT interval; **Imax** = maximum effect of ibutilide on QT; **EC_{50}** = serum ibutilide concentration required to achieve 50% of the maximum effect QT occurs; **Kout** = first order rate constant; **IOV**= Inter-occasion variability; **ω** = Inter-individual variability (omega), **σ** = Residual variability (sigma), **PROP** = Proportional, **RSE** = Residual standard error, **CI** = Confidence interval.

3.5.1 Biomarker Model

A sub-set of a linear model, direct and indirect models were attempted to describe serum miR-362-3p. Efforts to describe the influences of serum miR-362-3p in the circulation on the PD model parameters through a semi-mechanistic model were not successful. The indirect response model to describe the expression of serum miR-362-3p observed within a is illustrated in Figure 11. The expression patterns of serum miR-362-3p observed within as the study groups is displayed in Figure 12. Due to the small sample size, availability of the baseline of serum miR-362-3, and collections time was limitations for the dataset, this approached failed. Therefore, a sub-set of the liner and direct model was attempted, but none of the serum miR-362-3p model parameters were predicted by the model; thus, a covariate analysis approach was used.

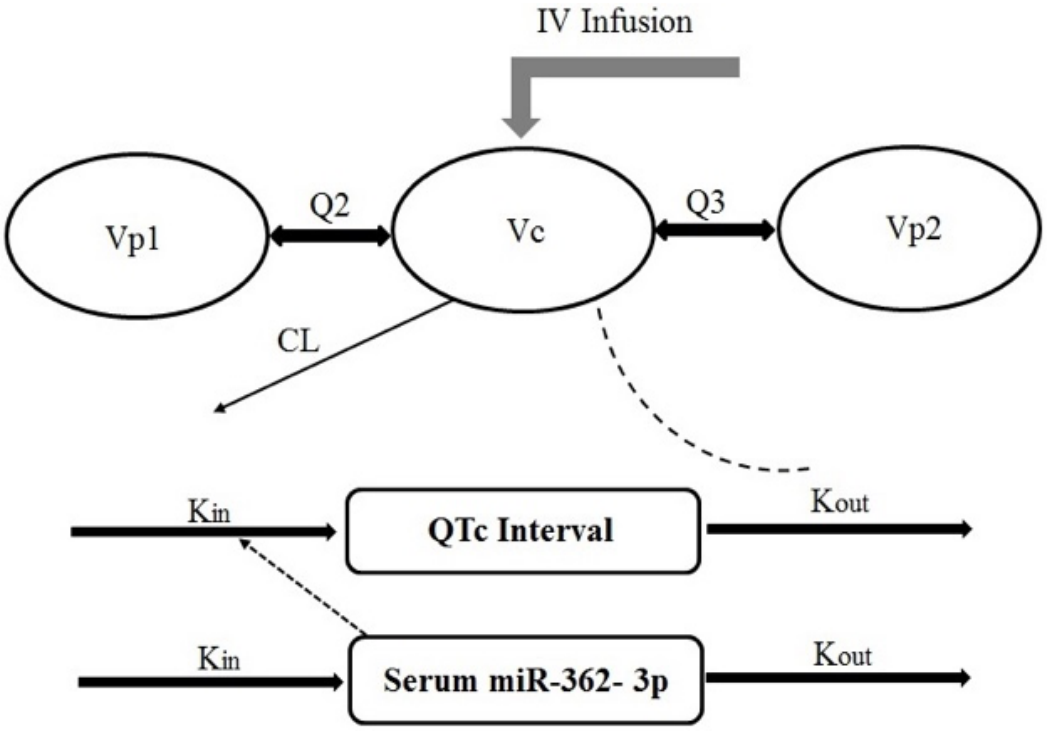

Figure 11. Schematic picture for the biomarker model linked to the PKPD model

Note. Kin= denotes the zero-order rate constant; Kout= denotes the first-order rate constant

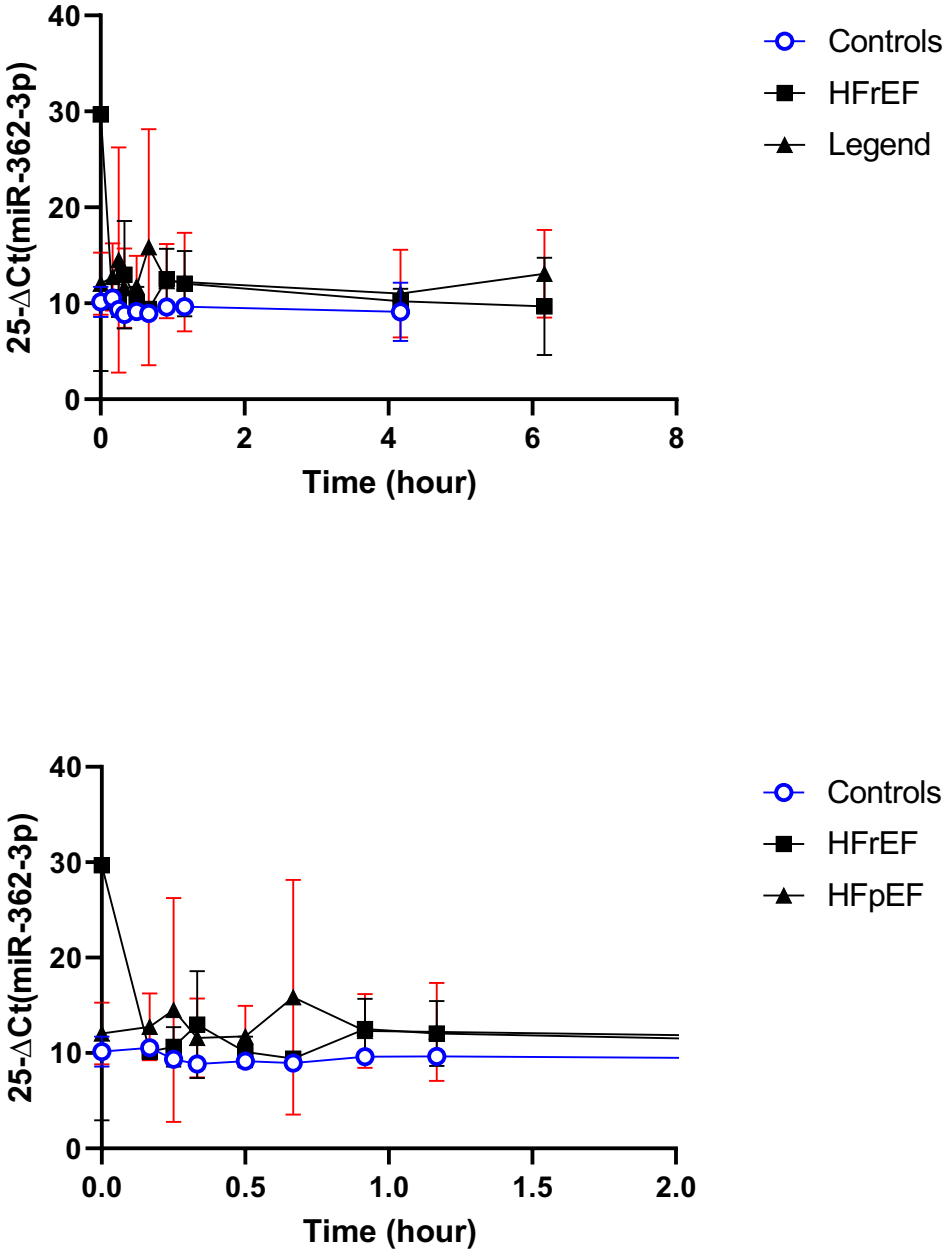

Figure 12. **The expressions of serum miR-362-3p (CT-25) vs Time (hrs.) in three groups of heart failure subjects**

3.5.2 Covariate Analysis— Model

An alternative approach with miR-362-3p in the serum was included with other covariates that potentially influence PK-PD model parameters, as listed in Table 6. The covariate selection process was done using stepwise selection procured on Imax and IC_{50} parameters, where forward inclusion resulted in the PK-PD model identifying circulating miR-362-3p expression in serum and myocardial infarction as a significant covariate influencing Imax parameter (ΔOFV -16.03, -15.09, $p<0.05$).

Overall, the constructed PK-PD model's performance was improved compared to the base PK-PD model, and the included covariates of the un-explained variability in the population. Compared to base model the unexplained inter-patient variability in the final covariate PK-PD model decreased from 11.8% to 9.7% for Imax which significantly reduced the OBJ -5.2. Overall, the performance of the constructed covariate PK-PD model was acceptable compared to the base model. The final PK-PD model estimates, and covariate-parameter relationships are summarized in Table 6.

Table 6. Summary of covariates in the pharmacokinetic/pharmacodynamic (PK/PD) modeling

	OBJ	Delta OBJ	EC50	Emax	P Values
BASE MODEL	2243.65				
miR-362-3p on Imax	2227.62	-16.04	0.32	0.10	<0.05
miR-362-3p on IC50	2235.87	-7.76	0.48	0.12	<0.05
HFG on Imax	2243.65	0.00	0.35	0.11	ns
HFG on IC50	2252.39	8.74	0.25	0.10	ns
SEX on Imax	2243.57	-0.08	0.35	0.12	ns
SEX on IC50	2243.62	-0.04	0.38	0.11	ns
RACE on Imax	2241.35	-2.30	0.43	0.13	ns
RACE on IC50	2243.64	-0.01	0.36	0.11	ns
Weight on Imax	2243.63	-0.02	0.35	107.00	ns
Weight on IC50	2243.65	0.00	0.38	0.11	ns
AGE on Imax	2243.65	0.00	0.35	0.11	ns
AGE on IC50	2242.80	-0.85	1.57	0.11	ns
DM on Imax	2239.15	-4.50	0.38	0.13	<0.05
DM on IC50	2241.99	-1.67	0.47	0.11	ns
MI on Imax	-15.97	-15.97	0.30	0.15	<0.05
MI on IC50	2243.61	-0.04	0.38	0.11	ns
LVEF on Imax	2243.65	0.00	0.35	0.11	ns
LVEF on IC50	2243.65	0.00	0.35	0.11	ns
BB Imax	2243.65	0.00	0.11	0.35	ns
BB IC50	2243.65	0.00	0.29	0.11	ns
LD on Imax	2243.65	-1.25	0.12	0.37	ns
LD on IC50	2243.65	-3.72	0.36	0.12	ns
ACE on Imax	2243.65	-0.36	0.24	0.11	ns
ACE on IC50	2242.07	-1.59	0.24	0.11	ns

Note: **ΔOFV** is the difference in objective function values between base and covariate model; **DM**= Diabetes mellitus; **MI**= Myocardial infractions; **LEVF**= Left vehicular fractions **BB**= Beta-blocker; **ACE**= ACE inhibitors; **LD**=Loop

Table 7. Forward Selections

Base Model 1	**OBJ**	**Delta OBJ**	**IC50**	**Imax**
miR-362-3p on Imax	**2227.62**		**0.32**	**0.10**
miR-362-3p + MI on Imax	2222.10	-5.52	0.26	0.09
miR-362-3p + MI on Imax + miR-362-3p on IC50	2221.91	-0.20	0.24	0.09
miR-362-3p, MI + DM on Imax	2222.10	0.00	0.26	0.09

Note. Most significates were miR-362-2p which were kept in the model while testing others.

Model Evaluation

The individual QT intereval vs time models (Figure 13) demonstrated a good descriptive of model predictions wihtout clear mis-specifications'. The predictive performance of the final PK-PD model was evaluated using visual predictive check. The VPC plots determined to be acceptable as the most observed data points contained in the 90% prediction interval (5^{th} - 95^{th} percentiles) of the model (Figure 14). Moreover, the final covariate PK-PD parameter estimates for both fixed and random-effect models agreed with the corresponding median estimated obtained from bootstrap analysis. This indicates the high predictive performance of the final model parameter estimates (Table 8).

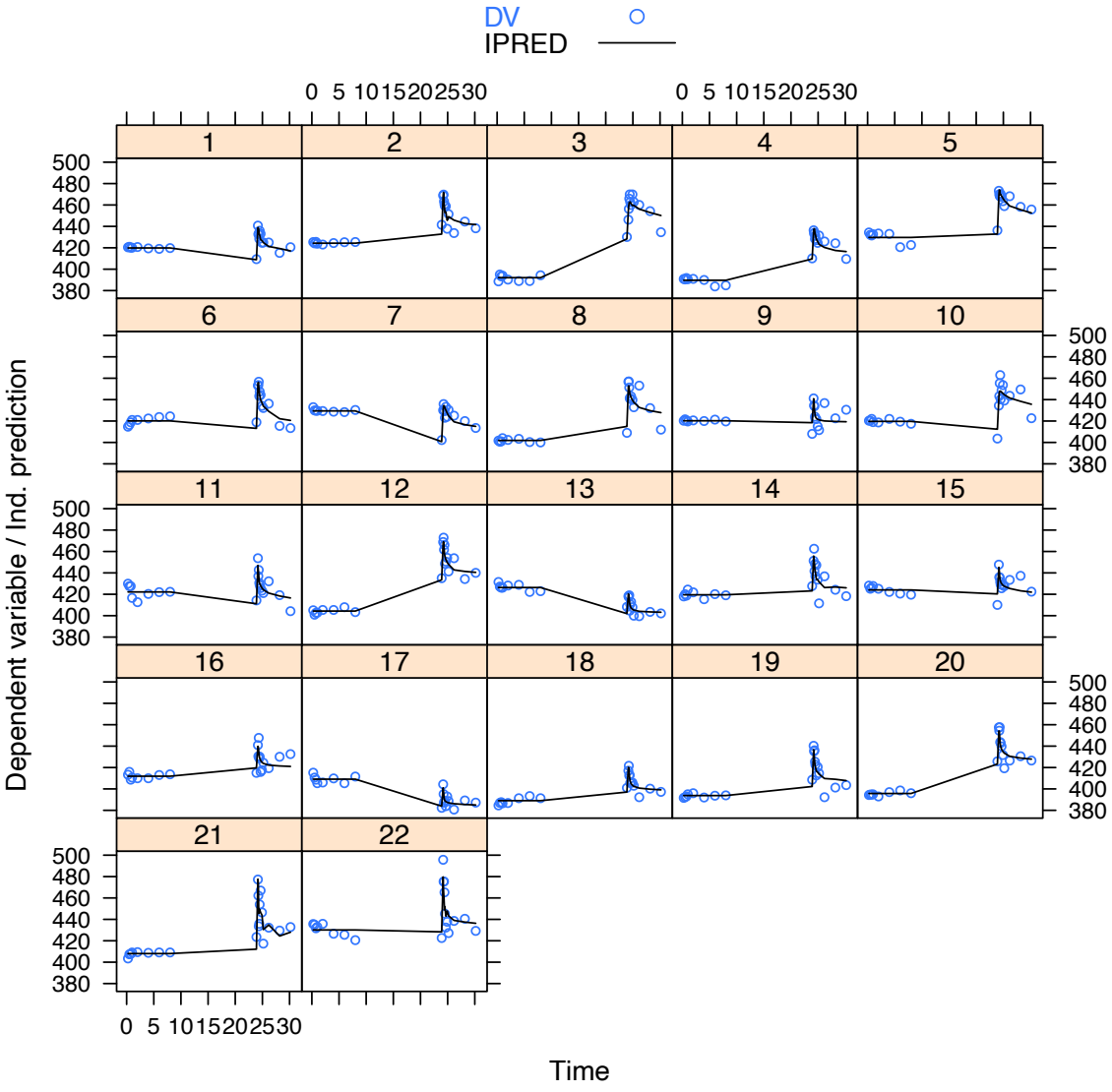

Figure 13. Individual plots for the final PK-PD model outputs

Note. Open circles are observed QT interval. Solid lines are individual predicted QT intervals.

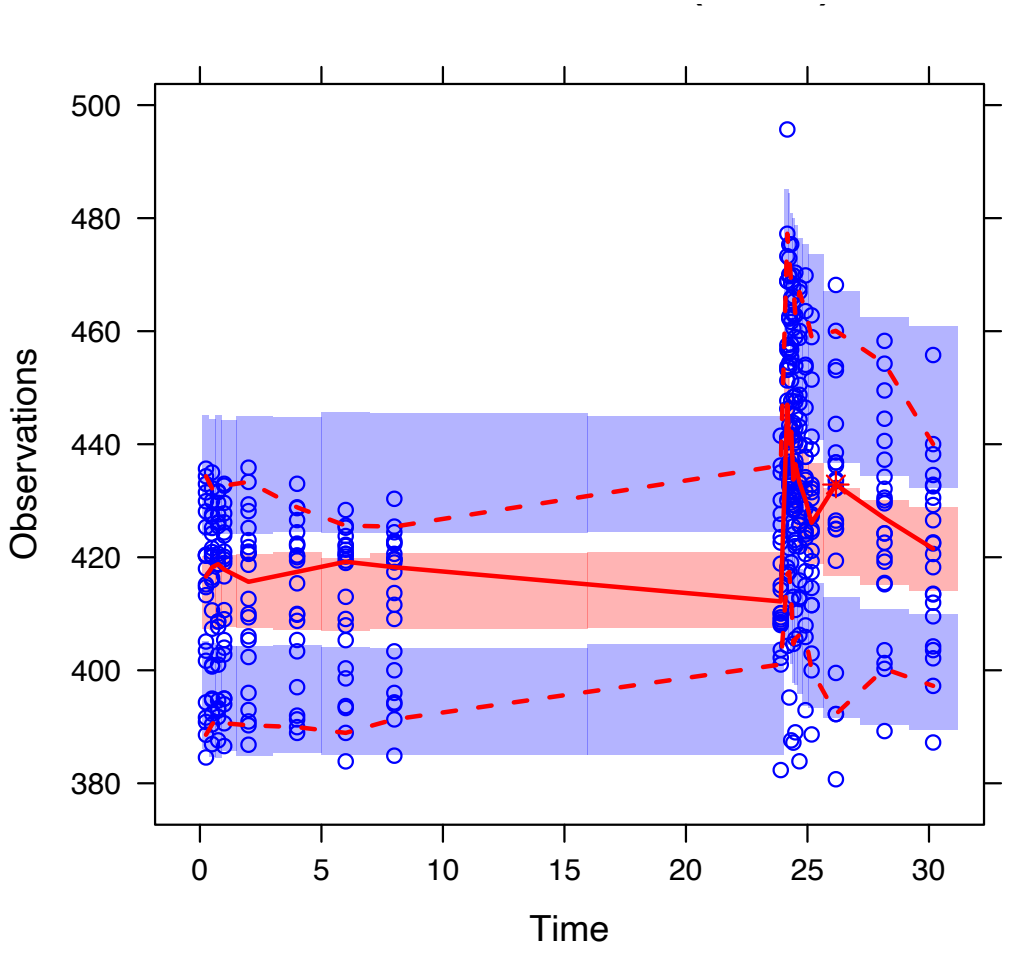

Figure 14. Visual predictive checks (VPC) of final the PK-PD model

Note. QT intervals (ms) are represented by open circles. The observed 5% and 95% percentiles are presented with dashed red lines, and the 95% confidence intervals for the corresponding model predicted percentiles as described by semitransparent blue fields.

Table 8. Summary of the final Covariate PK/PD parameters estimate

Parameter	Population Estimates (RES%)
$Imax_{(\%)}$	9 (8.9%)
IC_{50} (ng/mL)	0.26 (8.4%)
Baseline QT (ms)	414 (0.5%)
$K_{out\ (hr^{-1})}$	11.2 (1.4%)
ω K_{out}	0.324 (31.2%)
ω IC_{50}	1.46 (9%)
ω Baseline QT	0 FIX
IOV Variance	0.00107(0%)
IOV Variance	0.00107(5%)
σ PROP	0.00019 (8 %)

Note. * Based on Percentiles. **Base**, pre-ibutilide dose QT interval; **Imax** = maximum effect of ibutilide on QT; IC_{50} = serum ibutilide concentration required to achieve 50% of the maximum effect QT occurs; **Kout** = first order rate constant; **IOV**, Inter-occasion variability; **ω** = Inter-individual variability (omega), **σ** = Residual variability (sigma), **PROP** = Proportional, **RES** = Residual standard error, **CI** = Confidence interval.

CHAPTER 4. DISCUSSION

In the present study, the contribution of serum miR-362-3p to drug-associated QT interval changes in patients with heart failure was investigated. For this purpose, a PK-PD model was developed to describe the relationship between ibutilide concentration and QTc changes and determine the contribution of miR-362-3p expression and other potential covariates' variability with ibutilide-induced QT interval lengthening.

The PK and PD data used in the current project were obtained from a previous clinical trial that assessed patients' susceptibility with HFpEF to ibutilide-induced QT interval prolongation. (Tisdale, et al. 2020) Based on a nonlinear mixed effect model approach, the population pharmacokinetic model described the serum ibutilide concentration vs. time profile. This was best described by a three compartmental model with a first-order elimination rate constant from the central compartment, consistent with previously published population PK model. (Z Zeng, et al. 2017)

The present study's outcome demonstrated that subjects with heart failure had a greater degree of ibutilide-induced QTc, with a mean Imax increase by 39% compared to the control group. Accordingly, HF patients (either HFrEF or HFpEF) had greater ibutilide-induced QT interval lengthening. In general, a QTc of higher than 500 ms or an increase in the QTc] greater than 60 ms is considered to confer an increased risk of TdP in an individual patient. (Heist, et al. 2005, Barnes, et al. 2010)

In this analyses the effect of serum miR-362-3p expression on ibutilide-induced QTc interval was evaluated as a potential covariate on IC50 and Imax. Overexpression of serum miR-362-3p was identified as a predictor of ibutilide sensitivity with an IC50 (ng/mL) 0.26 (8.4%) as compared to ibutilide base PD model parameters with an IC50 (ng/ml) 0.34 (21.7%)

Notablypatients with higher expression of serum miR-362-3p demonstrated lower IC50 associated with ibutilide induced QT. The specific mechanism determining the association between miR-362-3p expression and QT interval sensitivity remains unclear. One possible explanation is the reduction of potassium channels, thereby enhancing ibutilides effect. Furthermore, ibutilide might have a possible involvement in regulating miR-362-3p expression.(Rodrigues, et al. 2011) The authors evaluated 19 drugs' involvement in expressing ten different miRNAs in four different cell lines. It was found that all ten miRNAs were differentially expressed, depending on the type of drug administered. They concluded that several drugs might be associated with alteration of miRNA expression. Lastly, the changes noticed in ibutilide response could be related to either a significant increase in releasing cellular miRNAs to circulation or significant disposition of miRNAs from circulation, resulting in an alteration of circulating miR-362-3p.

The results of the covariate analysis concluded that erum miR-362-3p expression and a history of myocardial infarction were significant predictors on Imax . This indicates that subjects with a history of myocardial infarction or high expressions of serum miR-362-3p may be at an increased risk to ibutilide - induced QT interval prolongation.

The study had limitations including the small sample size. Thus the analysis may have been underpowered to detect clinically relevant statistical differences in covariates or outcome measures. Secondly, inter-intra variations between HF subgroups with elapsed time between the initial diagnosis and the impact of other morbidities were not evaluated. Furthermore, serum miR-362-3p expression levels may be influenced by other pathways, pathophysiological signaling, or underlying mechanisms that could not be assessed in the present study.

This is supported by previous lab work data, which has demonstrated that miR-362-3p expression reduced hERG regulation and may mediate the involvement in drug-induced QT interval lengthening (Assiri, et al. 2019). However, the definite mechanism of the association between miR-362-3p expression and the drug target remains inconclusive. Consequently, future studies should be directed towards understanding the association between microRNA serum expression and QT interval changes. The assessment of such an association would explain the mechanism and contribution of miRNA in drug-induced QT interval lengthening to enhance theraptutic interventions.

Conclusion

In conclusion, an indirect response model has been developed to describe the effects of ibutilide concentrations on QT-intervals. While the planned semi-mechanistic model did not work due to the study's limitations; serum miR-362-3p expression was identified as a significant predictor effect for ibutilide-induced QT-interval prolongation. Thus, serum miR-362-3p expression in the circulations was a significant preditor of ibutilide sensitivity base on the IC50 parameter estimates. The potential utility of serum miR-362-3p as a biomarker to identify patients at the most significant risk of TdP warrants further investigation.

BIBLIOGRAPHY

Aarons, L. (1991). "Population pharmacokinetics: theory and practice." British journal of clinical pharmacology 32(6): 669-670.

Acunzo, M., Romano, G., Wernicke, D. and Croce, C.M. (2015). "MicroRNA and cancer--a brief overview." Adv Biol Regul 57: 1-9.

Baheti, G., Kiser, J.J., Havens, P.L. and Fletcher, C.V.,. (2011). "Plasma and intracellular population pharmacokinetic analysis of tenofovir in HIV-1-infected patients." Antimicrob Agents Chemother 55(11): 5294-5299.

Agoram, B. M., Martin, S. W., & van der Graaf, P. H. (2007). The role of mechanism-based pharmacokinetic–pharmacodynamic (PK–PD) modelling in translational research of biologics. *Drug discovery today*, *12*(23-24), 1018-1024.

Ahnve, S. (1985). Correction of the QT interval for heart rate: review of different formulas and the use of Bazett's formula in myocardial infarction. *American heart journal*, *109*(3), 568-574.

Assiri, A.(2019) A., Mourad, N., Shao, M., Kiel, P., Liu, W., Skaar, T. C., & Overholser, B. R. MicroRNA 362-3p Reduces hERG-related Current and Inhibits Breast Cancer Cells Proliferation. *Cancer genomics & proteomics*, *16*(6), 433–442. https://doi.org/10.21873/cgp.20147

Azzouzi, A. R., Barret, E., Moore, C. M., Villers, A., Allen, C., Scherz, A., ... & Emberton, M. (2013). TOOKAD® S oluble vascular-targeted photodynamic (VTP) therapy: determination of optimal treatment conditions and assessment of effects in patients with localised prostate cancer. *BJU international*, *112*(6), 766-774.

Bagliani, G., Leonelli, F., & Padeletti, L. (2017). P wave and the substrates of arrhythmias originating in the atria. *Cardiac Electrophysiology Clinics*, *9*(3), 365-382.

Barnes, B. J. and J. M. Hollands (2010). "Drug-induced arrhythmias." Crit Care Med 38(6 Suppl). Bartel, D. P. (2009). "MicroRNAs: target recognition and regulatory functions." Cell 136(2): 215-233.

Bauer, R. J. (2019). "NONMEM Tutorial Part I: Description of Commands and Options, with Simple Examples of Population Analysis." CPT: pharmacometrics & systems pharmacology 8(8): 525-537.

Bayés-Genis, A., Lanfear, D.E., de Ronde, M.W., Lupón, J., Leenders, J.J., Liu, Z., Zuithoff, N.P., Eijkemans, M.J., Zamora, E., De Antonio, M. and Zwinderman, A.H. (2018). "Prognostic value of circulating microRNAs on heart failurerelated morbidity and mortality in two large diverse cohorts of general heart failure patients." Eur J Heart Fail 20(1): 67-75.

Bazett, H. C. (1920). An analysis of the time relations of electrocardiograms. *Heart*, *7*, 353-370.

Benet, L. Z. and P. Zia-Amirhosseini (1995). "Basic Principles of Pharmacokinetics." Toxicologic Pathology 23(2): 115-123.

Beuckelmann, D.J., Näbauer, M. and Erdmann, E. (1993). "Alterations of K+ currents in isolated human ventricular myocytes from patients with terminal heart failure." Circ Res 73(2): 379-385.

Bohnsack, M.T., Czaplinski, K. and GÖRLICH, D. (2004). "Exportin 5 is a RanGTP-dependent dsRNA-binding protein that mediates nuclear export of pre-miRNAs." Rna 10(2): 185-191.

Bonate, P. (2011). Pharmacokinetic-Pharmacodynamic Modeling and Simulation. USA, Springer

Broughton, J.P., Lovci, M.T., Huang, J.L., Yeo, G.W. and Pasquinelli, A.E. (2016). "Pairing beyond the Seed Supports MicroRNA Targeting Specificity." Mol Cell 64(2): 320-333.

Brummer, A. and J. Hausser (2014). "MicroRNA binding sites in the coding region of mRNAs: extending the repertoire of post-transcriptional gene regulation." Bioessays 36(6): 617-626.

Figg, W.D. and McLeod, H.L. eds. (2014). Handbook of Anticancer Pharmacokinetics and Pharmacodynamics. New York, Springer Science

Loscher, C.J., Hokamp, K., Wilson, J.H., Li, T., Humphries, P., Farrar, G.J. and Palfi, A.. (2008). "A common microRNA signature in mouse models of retinal degeneration." Exp Eye Res 87(6): 529-534.

Cai, X., Hagedorn, C.H. and Cullen, B.R. (2004). "Human microRNAs are processed from capped, polyadenylated transcripts that can also function as mRNAs." Rna 10(12): 1957-1966.

Calin, G.A., Dumitru, C.D., Shimizu, M., Bichi, R., Zupo, S., Noch, E., Aldler, H., Rattan, S., Keating, M., Rai, K. and Rassenti, L. (2002). "Frequent deletions and down-regulation of micro- RNA genes miR15 and miR16 at 13q14 in chronic lymphocytic leukemia." Proc Natl Acad Sci U S A 99(24): 15524-15529.

Campbell, J. E. and D Cohall (2017). Chapter 26 - Pharmacodynamics—A Pharmacognosy Perspective. Pharmacognosy. S. Badal and R. Delgoda. Boston, Academic Press: 513-525. Charles, B. (2014). "Population pharmacokinetics: An overview." Australian Prescriber 37: 210213.

Charles. C. (2014). *The comparative method: Moving beyond qualitative and quantitative strategies*. Univ of California Press.

Chistiakov, D.A., Orekhov, A.N. and Bobryshev, Y.V. (2016). "The role of miR-126 in embryonic angiogenesis, adult vascular homeostasis, and vascular repair and its alterations in atherosclerotic disease." J Mol Cell Cardiol 97: 47-55.

Choi, T. M., Chiu, C. H., & Chan, H. K. (2016). Risk management of logistics systems.

Czaplinski, A., & Steck, A. J. (2004). Immune mediated neuropathies. *Journal of neurology*, *251*(2), 127-137.

da Costa Martins, P.A., Bourajjaj, M., Gladka, M., Kortland, M., van Oort, R.J., Pinto, Y.M., Molkentin, J.D. and De Windt, L.J. (2008). "Conditional dicer gene deletion in the postnatal myocardium provokes spontaneous cardiac remodeling." Circulation 118(15): 1567-1576.

Dayneka, N.L., Garg, V. and Jusko, W.J. (1993). "Comparison of four basic models of indirect pharmacodynamic responses." J Pharmacokinet Biopharm 21(4): 457-478.

Denli, A.M., Tops, B.B., Plasterk, R.H., Ketting, R.F. and Hannon, G.J. (2004). "Processing of primary microRNAs by the Microprocessor complex." Nature 432(7014): 231-235.

Dessertenne, F. (1966). "[Ventricular tachycardia with 2 variable opposing foci]." Arch Mal Coeur Vaiss 59(2): 263-272.

Drew, B.J., Ackerman, M.J., Funk, M., Gibler, W.B., Kligfield, P., Menon, V., Philippides, G.J., Roden, D.M., Zareba, W. (2010). "Prevention of Torsade de Pointes in Hospital Settings." Circulation 121(8): 1047-1060.

Du, T. and P. D. Zamore (2005). "microPrimer: the biogenesis and function of microRNA." Development 132(21): 4645-4652.

Dumitru, D. (2002). *Electrodiagnostic medicine* (pp. 274-278). A. A. Amato, & M. J. Zwarts (Eds.). Philadelphia: Hanley & Belfus.

Endo, K., Weng, H., Kito, N., Fukushima, Y. and Iwai, N. (2013). "MiR-216a and miR-216b as markers for acute phased pancreatic injury." Biomed Res 34(4): 179-188.

Esterly, J. D., Christopher, C. Y., Viegers, S. M., & Rhee, Y. W. (2010). *U.S. Patent Application No. 29/341,946*.

Feng, X. J., & Jiang, L. (2006). Design and creation of superwetting/antiwetting surfaces. *Advanced Materials*, *18*(23), 3063-3078.

Fridericia, L. S. (1920). Die Systolendauer im Elektrokardiogramm bei normalen Menschen und bei Herzkranken. *Acta Medica Scandinavica*, *53*(1), 469-486.

Gobburu (2012). Pharmacometrics: Concepts and Applications to Drug Development. In Immunotherapy in Transplantation (eds). Landgraf, P., et al. (2007). "A mammalian microRNA expression atlas based on small RNA library sequencing." Cell 129(7): 1401-1414.

Gu, J., Xu, X., Feng, L., & Gu, X. (2014). Magnetic nanoparticle supported triphenylphosphine ligand for the Rh-catalyzed hydroformylation reaction. *Catalysis Communications*, *48*, 45-49.

Gu, W., Xu, Y., Xie, X., Wang, T., Ko, J.H. and Zhou, T. (2014). "The role of RNA structure at 5' untranslated region in microRNAmediated gene regulation." Rna 20(9): 1369-1375.

Gussak, I., Bjerregaard, P., Egan, T. M., & Chaitman, B. R. (1995). ECG phenomenon called the J wave: history, pathophysiology, and clinical significance. *Journal of electrocardiology*, *28*(1), 49-58.

Guzman-Villanueva, D., El-Sherbiny, I.M., Herrera-Ruiz, D., Vlassov, A.V. and Smyth, H.D. (2012). "Formulation approaches to short interfering RNA and MicroRNA: challenges and implications." J Pharm Sci 101(11): 4046-4066. Ha, M. and V. N.

Holford N. (2017). Pharmacodynamic principles and the time course of immediate drug effects. *Translational and clinical pharmacology*, *25*(4), 157–161.

Heist, E. K. and J. N. Ruskin (2005). "Drug-induced proarrhythmia and use of QTc-prolonging agents: clues for clinicians." Heart Rhythm 2(2 Suppl): 017.

Hu, J., Xu, Y., Hao, J., Wang, S., Li, C. and Meng, S. (2012). "MiR-122 in hepatic function and liver diseases." Protein Cell 3(5): 364371.

Huang, S.M., Abernethy, D.R., Wang, Y., Zhao, P. and Zineh. (2013). "The utility of modeling and simulation in drug development and regulatory review." J Pharm Sci 102(9): 2912-2923.

Hull, D. L. (1978). A matter of individuality. *Philosophy of science*, *45*(3), 335-360.

ICH, I. C. o. H. (2005). Technical Requirements for Registration of Pharmaceuticals for Human Use (ICH).

Indik, J. H., Pearson, E. C., Fried, K., & Woosley, R. L. (2006). Bazett and Fridericia QT correction formulas interfere with measurement of drug-induced changes in QT interval. *Heart rhythm*, *3*(9), 1003-1007.

Jusko, W. J. and H. C. Ko (1994). "Physiologic indirect response models characterize diverse types of pharmacodynamic effects." Clin Pharmacol Ther 56(4): 406-419.

Karlsson, M. O. and L. B. Sheiner (1993). "The importance of modeling interoccasion variability in population pharmacokinetic analyses." Journal of Pharmacokinetics and Biopharmaceutics 21(6): 735-750.

Keating, M. T., & Sanguinetti, M. C. (2001). Molecular and cellular mechanisms of cardiac arrhythmias. *Cell*, *104*(4), 569-580.

Keizer, R.J., Karlsson, M.O. and Hooker, A. (2013). "Modeling and Simulation Workbench for NONMEM: Tutorial on Pirana, PsN, and Xpose." CPT Pharmacometrics Syst Pharmacol 26(2): 24.

Kim (2014). "Regulation of microRNA biogenesis." Nat Rev Mol Cell Biol 15(8): 509-524.

Kirschner, M. B., Kao, S. C., Edelman, J. J., Armstrong, N. J., Vallely, M. P., van Zandwijk, N., & Reid, G. (2011). Haemolysis during sample preparation alters microRNA content of plasma. *PloS one*, *6*(9), e24145.

Klabunde, R. E. (2017). "Cardiac electrophysiology: normal and ischemic ionic currents and the ECG." Adv Physiol Educ 41(1): 29-37.

Lacey, L.F., Keene, O.N., Pritchard, J.F. and Bye, A. (1997). "Common noncompartmental pharmacokinetic variables: are they normally or log-normally distributed?" J Biopharm Stat 7(1): 171-178. Lala, M. and J. V. S.

Lee, R.C., Feinbaum, R.L. and Ambros, V. (1993). "The C. elegans heterochronic gene lin-4 encodes small RNAs with antisense complementarity to lin-14." Cell 75(5): 843-854.

Leptidis, S., el Azzouzi, H., Lok, S.I., de Weger, R., Kisters, N., Silva, G.J., Heymans, S., Cuppen, E., Berezikov, E., De Windt, L.J. and da Costa Martins, P. (2013). "A deep sequencing approach to uncover the miRNOME in the human heart." PLoS One 8(2): 27.

Lester, R.M., Paglialunga, S. and Johnson, I.A. (2019). "QT Assessment in Early Drug Development: The Long and the Short of It." Int J Mol Sci 20(6).

Levy, G. (1964). "Relationship between Elimination Rate of Drugs and Rate of Decline of Their Pharmacologic Effects." J Pharm Sci 53: 342-343.

Levy, G. (1966). "Kinetics of pharmacologic effects." Clinical Pharmacology & Therapeutics 7(3): 362-372.

Li, E.C., Esterly, J.S., Pohl, S., Scott, S.D. and McBride, B.F. (2010). "Drug-induced QT-interval prolongation: considerations for clinicians." Pharmacotherapy 30(7): 684-701.

Li, Y. and K. V. Kowdley (2012). "MicroRNAs in common human diseases." Genomics Proteomics Bioinformatics 10(5): 246-253.

Limpert, E., Stahel, W. A., & Abbt, M. (2001). Log-normal distributions across the sciences: keys and clues: on the charms of statistics, and how mechanical models resembling gambling machines offer a link to a handy way to characterize log-normal distributions, which can provide deeper insight into variability and probability—normal or log-normal: that is the question. *BioScience*, *51*(5), 341-352.

Lindbom, L., Pihlgren, P. and Jonsson, N. (2005). "PsN-Toolkit--a collection of computer intensive statistical methods for non-linear mixed effect modeling using NONMEM." Comput Methods Programs Biomed 79(3): 241-257.

Lo, R. and H. H. Hsia (2008). "Ventricular Arrhythmias in Heart Failure Patients." Cardiology Clinics 26(3): 381-403.

Locati, E.T., Bagliani, G. and Padeletti, L. (2017). "Normal Ventricular Repolarization and QT Interval: Ionic Background, Modifiers, and Measurements." Card Electrophysiol Clin 9(3): 487-513. Loscher,

Luo, Y., Su, B. O., Currie, W. S., Dukes, J. S., Finzi, A., Hartwig, U., ... & Pataki, D. E. (2004). Progressive nitrogen limitation of ecosystem responses to rising atmospheric carbon dioxide. *Bioscience*, *54*(8), 731-739.

Mager, D.E., Wyska, E. and Jusko, W.J. (2003). "Diversity of mechanism-based pharmacodynamic models." Drug Metab Dispos 31(5): 510-518.

Mancino, L., Sbroscia, M., Gianani, I., Roccia, E., & Barbieri, M. (2017). Quantum simulation of single-qubit thermometry using linear optics. *Physical Review Letters*, *118*(13), 130502.

Manion, A. S., Ahnve, S. T. A. F. F. A. N., Gilpin, E. L. I. Z. A. B. E. T. H., Henning, H. A. R. T. M. U. T., Goldberger, A. L., Collins, D. A. N. I. E. L., ... & Ross Jr, J. (1985). Prognosis after extension of myocardial infarct: the role of Q wave or non-Q wave infarction. *Circulation*, *71*(2), 211-217.

Marquez, R. T. and A. P. McCaffrey (2008). "Advances in microRNAs: implications for gene therapists." Human gene therapy 19(1): 27-38.

Marroni, F., Pfeufer, A., Aulchenko, Y.S., Franklin, C.S., Isaacs, A., Pichler, I., Wild, S.H., Oostra, B.A., Wright, A.F., Campbell, H. and Witteman, J.C. (2009). "A genome-wide association scan of RR and QT interval duration in 3 European genetically isolated populations: the EUROSPAN project." Circulation. Cardiovascular genetics 2(4): 322-328.

Meibohm, B., Beierle, I., & Derendorf, H. (2002). How important are gender differences in pharmacokinetics. *Clinical pharmacokinetics*, *41*(5), 329-342.

Mould, D. R. and R. N. Upton (2012). "Basic Concepts in Population Modeling, Simulation, and Model-Based Drug Development." CPT: Pharmacometrics & Systems Pharmacology 1(9): 6.

Mould, D. R. and R. N. Upton (2013). "Basic Concepts in Population Modeling, Simulation, and Model-Based Drug Development—Part 2: Introduction to Pharmacokinetic Modeling Methods." CPT: Pharmacometrics & Systems Pharmacology 2(4): 38.

Mould, D. R., Holford, N. H., Schellens, J. H., Beijnen, J. H., Hutson, P. R., Rosing, H., ... & Ross, G. (2002). Population pharmacokinetic and adverse event analysis of topotecan in patients with solid tumors. *Clinical Pharmacology & Therapeutics*, *71*(5), 334-348.

Mourad NA, Assiri A, Shao M, Tisdale JE, Liu W, and Overholser BR. (2015). MicroRNA 362-3p expression is upregulated in patients with heart failure. Featured Poster Presentation at Heart Rhythm 36th Annual Scientific Sessions. Boston, MA.

Näbauer, M., Beuckelmann, D.J. and Erdmann, E. (1993). "Characteristics of transient outward current in human ventricular myocytes from patients with terminal heart failure." Circ Res 73(2): 386-394.

O'Brien, J., Hayder, H., Zayed, Y. and Peng, C. (2018). "Overview of MicroRNA Biogenesis, Mechanisms of Actions, and Circulation." Front Endocrinol 9(402).

O'Brien, J., Hayder, H., Zayed, Y., & Peng, C. (2018). Overview of microRNA biogenesis, mechanisms of actions, and circulation. *Frontiers in endocrinology*, *9*, 402.

Oliveto, S., Mancino, M., Manfrini, N. and Biffo, S. (2017). "Role of microRNAs in translation regulation and cancer." World journal of biological chemistry 8(1): 45-56.

Ovchinnikova, E.S., Schmitter, D., Vegter, E.L., ter Maaten, J.M., Valente, M.A., Liu, L.C., van der Harst, P., Pinto, Y.M., de Boer, R.A., Meyer, S. and Teerlink, J.R. (2016). "Signature of circulating microRNAs in patients with acute heart failure." Eur J Heart Fail 18(4): 414-423.

Paraskevi, A., Theodoropoulos, G., Papaconstantinou, I., Mantzaris, G., Nikiteas, N. and Gazouli, M. (2012). "Circulating MicroRNA in inflammatory bowel disease." J Crohns Colitis 6(9): 900-904.

Park, S.M., Lee, J., Seong, S.J., Park, J.G., Gwon, M.R., Lim, M.S., Lee, H.W., Yoon, Y.R., Yang, D.H., Kwon, K.I. and Han, S. (2014). "Population pharmacokinetic and pharmacodynamic modeling of transformed binary effect data of triflusal in healthy Korean male volunteers: a randomized, open-label, multiple dose, crossover study." BMC Pharmacology and Toxicology 15(1): 75.

Pasquinelli, A. E. (2012). "MicroRNAs and their targets: recognition, regulation and an emerging reciprocal relationship." Nat Rev Genet 13(4): 271-282.

Phan, B. C., Pal, A. A., Valencia, R. M., & Bollella, D. (2015). *U.S. Patent No. 9,133,024*. Washington, DC: U.S. Patent and Trademark Office.

Piotrovsky, V. (2005). "Pharmacokinetic-pharmacodynamic modeling in the data analysis and interpretation of drug-induced QT/QTc prolongation." The AAPS journal 7(3).

Ploeger, B. A., van der Graaf, P. H., & Danhof, M. (2009). Incorporating receptor theory in mechanism-based pharmacokinetic-pharmacodynamic (PK-PD) modeling. *Drug metabolism and pharmacokinetics*, *24*(1), 3-15.

Pritchard, C.C., Cheng, H.H. and Tewari, M. (2012). "MicroRNA profiling: approaches and considerations." Nat Rev Genet 13(5): 358-369.

Rabkin, S. W. (2017). The role matrix metalloproteinases in the production of aortic aneurysm. In *Progress in molecular biology and translational science* (Vol. 147, pp. 239-265). Academic Press.

Rabkin, S. W., & Cheng, X. B. (2015). Nomenclature, categorization and usage of formulae to adjust QT interval for heart rate. *World Journal of Cardiology*, *7*(6), 315.

RAUTAHARJU, P. M., & ZHANG, Z. M. (2002). Linearly scaled, rate-invariant normal limits for QT interval: Eight decades of incorrect application of power functions. *Journal of cardiovascular electrophysiology*, *13*(12), 1211-1218.

Rautaharju, P. M., Surawicz, B., & Gettes, L. S. (2009). AHA/ACCF/HRS recommendations for the standardization and interpretation of the electrocardiogram: part IV: the ST segment, T and U waves, and the QT interval: a scientific statement from the American Heart Association Electrocardiography and Arrhythmias Committee, Council on Clinical Cardiology; the American College of Cardiology Foundation; and the Heart Rhythm Society: endorsed by the International Society for Computerized Electrocardiology. *Circulation*, *119*(10), e241-e250.

Rautaharju, P. M., Zhang, Z. M., Prineas, R., & Heiss, G. (2004). Assessment of prolonged QT and JT intervals in ventricular conduction defects. *The American journal of cardiology*, *93*(8), 1017-1021.

Reid, G., Kirschner, M.B. and van Zandwijk, N. (2011). "Circulating microRNAs: Association with disease and potential use as biomarkers." Crit Rev Oncol Hematol 80(2): 193-208.

Roden, D. M. (2008). "Cellular basis of drug-induced torsade's de pointes." Br J Pharmacol 154(7): 1502-1507.

Rodrigues, A.C., Li, X., Radecki, L., Pan, Y.Z., Winter, J.C., Huang, M. and Yu, A.M.(2011) MicroRNA expression is differentially altered by xenobiotic drugs in different human cell lines. Biopharm Drug Dispos 32(6):355-67.

Romaine, S.P., Tomaszewski, M., Condorelli, G. and Samani, N.J. (2015). "MicroRNAs in cardiovascular disease: an introduction for clinicians." Heart 101(12): 921-928.

Rusu, D., Dali, L., Fortuna, B., Grobelnik, M., & Mladenic, D. (2007, October). Triplet extraction from sentences. In *Proceedings of the 10th International Multiconference" Information Society-IS* (pp. 8-12).

Sagie, A., Larson, M. G., Goldberg, R. J., Bengtson, J. R., & Levy, D. (1992). An improved method for adjusting the QT interval for heart rate (the Framingham Heart Study). *The American journal of cardiology*, *70*(7), 797-801.

Sanguinetti, M.C., Jiang, C., Curran, M.E. and Keating, M.T. (1995). "A mechanistic link between an inherited and an acquired cardiac arrhythmia: HERG encodes the IKr potassium channel." Cell 81(2): 299-307.

Schulte, C., Westermann, D., Blankenberg, S. and Zeller, T. (2015). "Diagnostic and prognostic value of circulating microRNAs in heart failure with preserved and reduced ejection fraction." World journal of cardiology 7(12): 843860.

Schwarz, D.S., Hutvágner, G., Du, T., Xu, Z., Aronin, N. and Zamore, P.D. (2003). "Asymmetry in the assembly of the RNAi enzyme complex." Cell 115(2): 199-208.

Shao, M., Odell, J., Humbert, M., Yu, T., & Xia, Y. (2013). Electrocatalysis on shape-controlled palladium nanocrystals: oxygen reduction reaction and formic acid oxidation. *The Journal of Physical Chemistry C*, *117*(8), 4172-4180.

Sharma, A. and W. J. Jusko (1998). "Characteristics of indirect pharmacodynamic models and applications to clinical drug responses." British journal of clinical pharmacology 45(3): 229-239.

Sharma, S. and H.-C. Lu (2018). "microRNAs in Neurodegeneration: Current Findings and Potential Impacts." Journal of Alzheimer's disease & Parkinsonism 8(1): 420.

Stanski, D. R., & Maitre, P. O. (1990). Population Pharmacokinetics and Pharmacodynamics of ThiopentalThe Effect of Age Revisited. *Anesthesiology: The Journal of the American Society of Anesthesiologists*, *72*(3), 412-422.

Straus, S. E., Gelb, L. D., ... & Weinberg, A. (2005). A vaccine to prevent herpes zoster and postherpetic neuralgia in older adults. *New England Journal of Medicine*, *352*(22), 2271-2284.

Strauss, E., Sherman, E. M., & Spreen, O. (2006). *A compendium of neuropsychological tests: Administration, norms, and commentary*. American Chemical Society.

Sun, H., Fadiran, E.O., Jones, C.D., Lesko, L., Huang, S.M., Higgins, K., Hu, C., Machado, S., Maldonado, S., Williams, R. and Hossain, M. (1999). "Population pharmacokinetics. A regulatory perspective." Clin Pharmacokinet 37(1): 41-58.

Sygitowicz, G., Tomaniak, M., Błaszczyk, O., Kołtowski, Ł., Filipiak, K.J. and Sitkiewicz, D. (2015). "Circulating microribonucleic acids miR-1, miR-21 and miR-208a in patients with symptomatic heart failure: Preliminary results." Archives of Cardiovascular Diseases 108(12): 634-642.

Sygitowicz, G., Tomaniak, M., Błaszczyk, O., Kołtowski, Ł., Filipiak, K. J., & Sitkiewicz, D. (2015). Circulating microribonucleic acids miR-1, miR-21 and miR-208a in patients with symptomatic heart failure: preliminary results. *Archives of Cardiovascular Diseases*, *108*(12), 634-642.

Theodoropoulos, G. E., Saridakis, V., Karantanos, T., Michalopoulos, N. V., Zagouri, F., Kontogianni, P., ... & Zografos, G. C. (2012). Toll-like receptors gene polymorphisms may confer increased susceptibility to breast cancer development. *The Breast*, *21*(4), 534-538.

Thomas, M., Maconochie, J.G. and Fletcher, E. (1996). "The dilemma of the prolonged QT interval in early drug studies." British journal of clinical pharmacology 41(2): 77-81.

Thum, T., Catalucci, D., & Bauersachs, J. (2008). MicroRNAs: novel regulators in cardiac development and disease. *Cardiovascular research*, *79*(4), 562-570.

Tisdale JE, Jaynes HA, Overholser BR, Sowinski KM, Fisch MD, Rodgers JE, Aldemerdash A, Hsu CC, Wang N, Muensterman ET, Rao VU, Kovacs RJ. (2020). Enhanced Response to Drug-Induced QT Interval Lengthening in Patients with Heart Failure with Preserved Ejection Fraction. J Card Fail, 26(9):781-785.

Tisdale, J. E., Chung, M. K., Campbell, K. B., Hammadah, M., Joglar, J. A., Leclerc, J., ... & American Heart Association Clinical Pharmacology Committee of the Council on Clinical Cardiology and Council on Cardiovascular and Stroke Nursing. (2020). Drug-Induced Arrhythmias: A Scientific Statement From the American Heart Association. *Circulation*, CIR-0000000000000905.

Tisdale, J.E., Overholser, B.R., Sowinski, K.M., Wroblewski, H.A., Amankwa, K., Borzak, S., Kingery, J.R., Coram, R., Zipes, D.P., Flockhart, D.A. and Kovacs, R.J. (2008). "Pharmacokinetics of ibutilide in patients with heart failure due to left ventricular systolic dysfunction." Pharmacotherapy 28(12): 1461-1470.

Tomaselli, G. F. and E. Marbán (1999). "Electrophysiological remodeling in hypertrophy and heart failure." Cardiovascular Research 42(2): 270-283.

Tomaszewski, M., Condorelli, G., & Samani, N. J. (2015). MicroRNAs in cardiovascular disease: an introduction for clinicians. *Heart*, *101*(12), 921-928.

Ultimo, S., Zauli, G., Martelli, A.M., Vitale, M., McCubrey, J.A., Capitani, S. and Neri, L.M. (2018). "Cardiovascular disease-related miRNAs expression: potential role as biomarkers and effects of training exercise." Oncotarget 9(24): 17238-17254.

Upton, R. N. and D. R. Mould (2014). "Basic concepts in population modeling, simulation, and model-based drug development: part 3-introduction to pharmacodynamic modeling methods." CPT: pharmacometrics & systems pharmacology 3(1): e88-e88.

van Wijnen, A.J., Van De Peppel, J., Van Leeuwen, J.P., Lian, J.B., Stein, G.S., Westendorf, J.J., Oursler, M.J., Im, H.J., Taipaleenmäki, H., Hesse, E. and Riester, S. (2013). "MicroRNA functions in osteogenesis and dysfunctions in osteoporosis." Curr Osteoporos Rep 11(2): 72-82.

Van Wynsberghe, P.M., Chan, S.P., Slack, F.J. and Pasquinelli, A.E. (2011). "Analysis of microRNA expression and function." Methods Cell Biol 106: 219-252.

Vandenberg, J.I., Perry, M.D., Perrin, M.J., Mann, S.A., Ke, Y. and Hill, A.P. (2012). "hERG K(+) channels: structure, function, and clinical significance." Physiol Rev 92(3): 1393-1478.

Vandenberk, B., Vandael, E., Robyns, T., Vandenberghe, J., Garweg, C., Foulon, V., ... & Willems, R. (2016). Which QT correction formulae to use for QT monitoring?. *Journal of the American Heart Association*, *5*(6), e003264.

Vandenberk, B., Vandael, E., Robyns, T., Vandenberghe, J., Garweg, C., Foulon, V., ... & Willems, R. (2016). Which QT correction formulae to use for QT monitoring?. *Journal of the American Heart Association*, *5*(6), e003264.

Wang, J., Yang, L.Z., Zhang, J.S., Gong, J.X., Wang, Y.H., Zhang, C.L., Chen, H. and Fang, X.T. (2018). "Effects of microRNAs on skeletal muscle development." Gene 668: 107113.

Wei, X.J., Han, M., Yang, F.Y., Wei, G.C., Liang, Z.G., Yao, H., Ji, C.W., Xie, R.S., Gong, C.L. and Tian, Y. (2015). "Biological significance of miR-126 expression in atrial fibrillation and heart failure." Brazilian Journal of Medical and Biological Research 48: 983-989.

Wu, L., Rajamani, S., Li, H., January, C.T., Shryock, J.C. and Belardinelli, L. (2009). "Reduction of repolarization reserve unmasks the proarrhythmic role of endogenous late Na(+) current in the heart." Am J Physiol Heart Circ Physiol 297(3): 10.

Wu, L., Rajamani, S., Li, H., January, C. T., Shryock, J. C., & Belardinelli, L. (2009). Reduction of repolarization reserve unmasks the proarrhythmic role of endogenous late Na+ current in the heart. *American Journal of Physiology-Heart and Circulatory Physiology*, *297*(3), H1048-H1057.

Xiao, M., Li, J., Li, W., Wang, Y., Wu, F., Xi, Y., Zhang, L., Ding, C., Luo, H., Li, Y. and Peng, L. (2017). "MicroRNAs activate gene transcription epigenetically as an enhancer trigger." RNA Biol 14(10): 1326-1334.

Yasuda, C., Yasuda, S., Yamashita, H., Okada, J., Hisada, T. and Sugiura, S. (2015). "The human ether-a-go-go-related gene (hERG) current inhibition selectively prolongs action potential of midmyocardial cells to augment transmural dispersion." J Physiol Pharmacol 66(4): 599-607.

Zauli, G., Martelli, A. M., Vitale, M., Sacchetti, G., Gonelli, A., & Neri, L. M. (2018). Oxidative stress: role of physical exercise and antioxidant nutraceuticals in adulthood and aging. *Oncotarget*, *9*(24), 17181.

Zeng, Z., Wang, L.I., Hua, L.U., Jiang, J., Pang, H., Huang, Y., Li, Y. and Tian, L. (2017). "Population Pharmacokinetic/Pharmacodynamics Modeling of Ibutilide in Chinese Healthy Volunteers and Patients With Atrial Fibrillation (AF) and/or Atrial Flutter (AFL)." Clin Ther 39(7): 1320-1335.

Zhou, S.S., Jin, J.P., Wang, J.Q., Zhang, Z.G., Freedman, J.H., Zheng, Y. and Cai, L. (2018). "miRNAS in cardiovascular diseases: potential biomarkers, therapeutic targets and challenges." Acta Pharmacologica Sinica 39(7): 1073-1084. Sheiner, L. B., Rosenberg, B., & Melmon, K. L. (1972). Modelling of individual pharmacokinetics for computer-aided drug dosage. *Computers and Biomedical Research*, *5*(5), 441-459.